REPORT ON IP cum RES, SP & MAGNETIC SURVEY IN

BARGUR BLOCK

DISTRICT: KRISHNAGIRI. STATE: TAMIL NADU

FOR

GOLD MINERALIZATION.

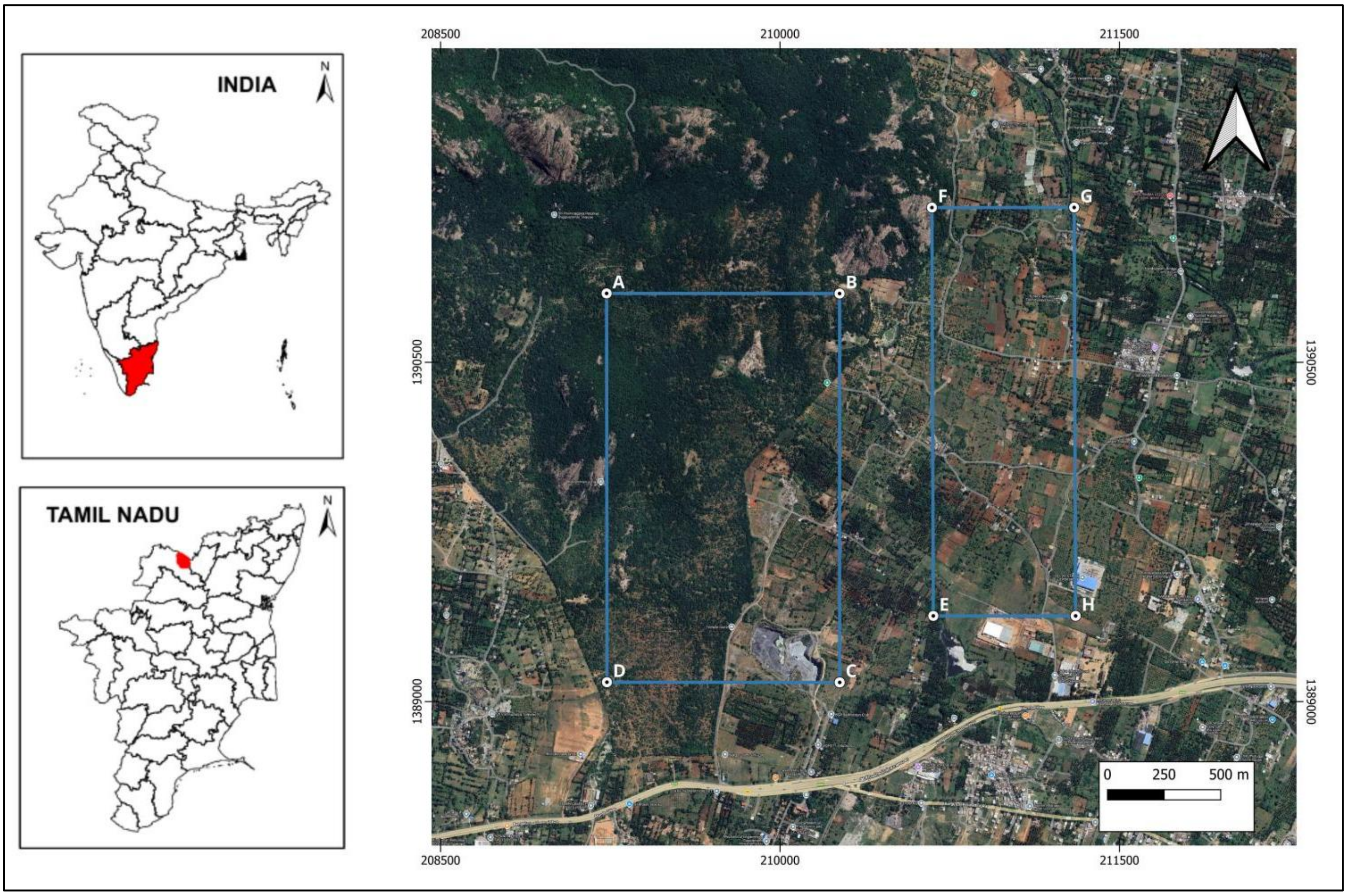

SEP-2025

मिनरल एक्सप्लोरेशन एंड कंसल्टेंसी लिमिटेड

खान मंत्रालय, भारत सरकार का उद्यम, मिनीरत्न- । सीपीएसई

MINERAL EXPLORATION AND CONSULTANCY LIMITED.

Ministry of Mines, Govt of India Enterprise, MINIRATNA-I CPSE

An ISO 9001:2015, 14001:2015 & 45001:2018 Certified Company

Page

1.0 INTRODUCTION

Mineral Exploration & Consultancy Limited (MECL) formerly as Mineral Exploration Corporation Limited having its corporate office at Nagpur, Maharashtra is functioning under Ministry of Mines, Government of India with 100% holding for systematic exploration of minerals.

In view of the MMDR amendments act -2015, Minerals (Evidence of Mineral Contents) Rule 2015 and Mineral Auction Rule-2015, Ministry of Mines, MECL prepared proposal for G-4 level exploration of Bargur Block and submitted in the 43rd meeting of Technical-cum-Cost Committee (TCC) of NMET held on 28.07.2022 for approval. After detailed discussion TCC recommended it for approval of Executive Committee (EC) of NMET. The proposal was approved by EC in its 32nd meeting held on 20.12.2023 and approval received from NMET on 12.12.2023.

1.1 SCOPE OF WORK

Based on the evaluation of available geological data and reported known occurrence of the exploration scheme of Bargur G4 block, Krishnagiri District of Tamil Nadu is formulated with the following objectives:

Phase-I

- To carry out Geological & Structural mapping on 1:12,500 scale for demarcation of gold bearing formations (host rock) with the structural features to identify the surface manifestations and lateral disposition of the mineralized zones.
- To collect surface (Bedrock/soil/stream sediment) samples & analyse for Gold & Silver and associated minerals to identify the host rock.
- To carry out surface geophysical IP cum Resistivity, SP and Magnetic to demarcate potential areas for mineral targeting and giving sub-surface positive details of extension of concealed ore body.
- To carry out trenching/pitting work in the identified anomalous zones
- Based on the positive outcome of geological mapping, surface geochemical sample results, ground geophysical survey and trenching/pitting work scout drilling (500m in 5 Bhs) shall be carried out in the potential mineral bearing area to confirm the subsurface continuity of mineralisation.
- To estimate Reconnaissance resource (334) for Gold along with accessory elements if any as per UNFC norms and Minerals (Evidence of Mineral Content) Rules-2015 at G-4 level.

If phase-I exploration data will give positive results, 5 Nos. of scout boreholes may be drilled.

1.2 GEOLOGY OF THE AREA:

The Bargur block area is part of Bargur belt and lies in the southern end of Kolar Schist Belt. The Bargur belt of Tamil Nadu represents the southern extension of the eastern tail of Kolar schist belt. Hornblende schist amphibolite occurs in the southern part of the Kolar schist belt where it has been designated as Bargur series (Gopalakrishnan et al., op.cit.). These are included in the Kolar Group of Subramanian and Selvan (op.cit.)

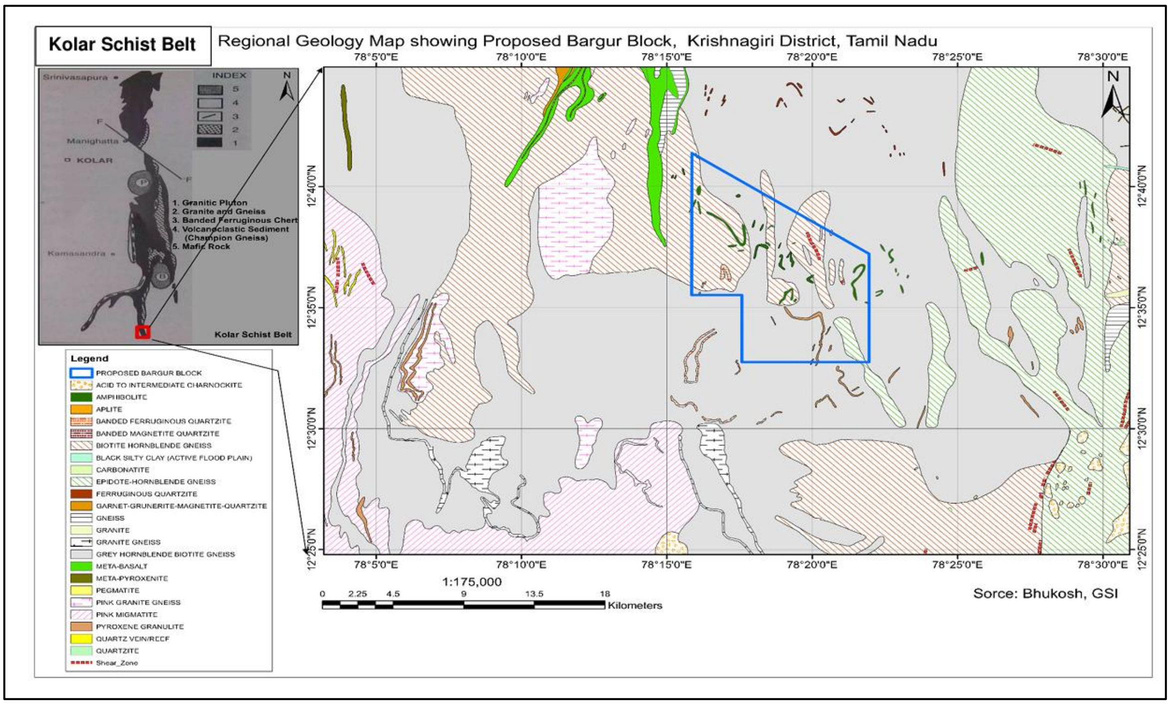

1.3 Regional geology:

The Bargur series (Formation) is made up of hornblende schist, amphibolite, banded iron formation and mica schist. The easternmost schist belt of Karnataka (Kolar schist belt) traced in a north - south direction extends at its southern end into the Dharampuri district of Tamil Nadu, where the belt splits up into two arms. Here, the rock types are the same as those of Kolar schist belt and include biotite and hornblende gneisses and amphibolites with banded ferruginous quartzite, quartzo-feldspathic gneiss and quartz-sericite schist. Banded Iron Formations consisting dominantly of quartz and iron oxides are significant components of the Bargur series. The common mineral constituents of the iron formation in amphibolite facies are quartz and magnetite with or without grunerite and cummingtonite. In granulite facies, the said mineral assemblage is added by hedenbergitic clinopyroxene, orthopyroxene and garnet. The iron formation represents a platformal environment of deposition (Naqvi and Rogers, op.cit.). Mafic granulites associated with the iron formations are meta igneous as indicated by the composition of the constituent magnetites. The content of Cr, Ni, Mn, V and Ti is lower in the magnetites of the iron formations than the magnetites of the mafic granulites (Subba Reddy and Prasad, 1982).

he generalized lithological succession of the area is given in the Table I.A. and location of the Bargur block area is shown Fig. No.1.

Table 1.1: **Regional Stratigraphic sequence of Litho units (After GSI)**

Age	Group	Litho-units
Archaean	Recent to Sub-recent	Soil/kankar
	Acid Intrusive	Quartz and Pegmatite veins
	Basic Intrusive	Dolerite Gabbro
	Peninsular Gneissic Complex	Migmatite Pyroxenite dyke
	Kolar Schist Belt	Amphibolite, Banded Iron Formation, Meta-chert

1.4 Geology of the Block:

General Geology:

The litho-units exposed in the area form a part of the Peninsular Gneissic Complex with lenses and enclaves of amphibolite and banded iron formation (in the form of ferruginous quartzite) and meta-chert of Kolar schist belt. The Peninsular Gneissic Complex is represented by migmatites which was earlier called as granite/gneiss/ granitoids. Migmatites form the major rock type of the area. The amphibolite and banded iron formations occur as enclaves within migmatite. The schist belt units are occurring as rafts within the migmatites. All these rock types are intruded by basic and ultrabasic dykes of dolerite/gabbro and pyroxenite composition and acid intrusive of Quartz and pegmatite veins. Two ancient/old workings for gold known as Sakalagunta and Bangaragunta located within Amphibolites in Bargur area.

2.0 BRIEF INTRODUCTION OF GEOPHYSICAL METHODS:

2.1 Induced Polarization:

Induce Polarization is the phenomena referred to build up of ionic charges in subsurface materials under the influence of electric field. There are two types survey method in IP

I. Time Domain.
II. Frequency Domain.

I. Time Domain: The normalised area under the decay curve is the most often measured type of time domain IP. Using the parameters listed in the adjacent graphic, the following equation may be used to represent it.
Essentially, chargeability (M) is the red region beneath the decay curve that has been normalised by the source voltage.

$$M = 1/V_p \int V_s (t)\, dt$$

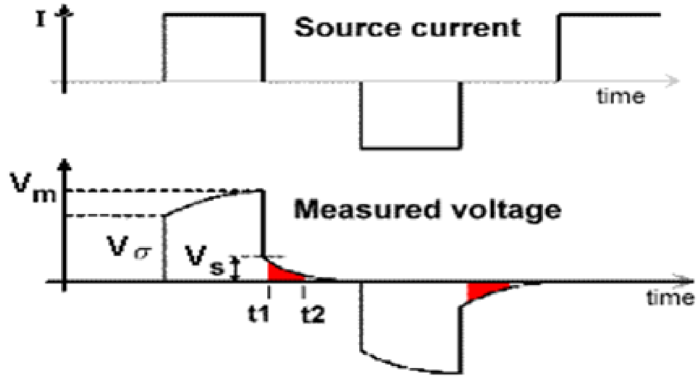

Fig. 2.1: Source current and voltage decay with respect to time in IP time domain method.

II. Frequency Domain: In frequency domain method the amplitude of potential is measured for two frequencies and it can be expressed as frequency effect. In this method the resulting data include i) DC resistivity ρ_{dc} and ii) ρ_{ac} for non-zero low frequency.
Frequency Effect can be expressed as following equation.

$$FE = (\rho_{ac} - \rho_{dc})/\rho_{ac}$$

Similar to resistivity method depth of investigation can be increased by increasing spread of the array.
All the different type of array in IP method has their advantages and disadvantages, so it is very crucial to select optimum array method considering our objective.

2.2 Self-Potential Method:

The Self Potential method is based on the surface measurement of natural potential differences resulting from electrochemical reactions in the subsurface. Typical SP anomalies may have amplitude of several hundred millivolts (mV) with respect to barren ground. They invariably exhibit a central -Ve anomaly and are stable over long periods of time. Field studies indicate that for a SP. Anomaly to occur its causative body must lie partially in a zone of oxidation. They are usually associated with deposits of metallic sulphides, magnetite or graphite.

A widely-accepted mechanism of self-potential requires the causative body to straddle the water table. Below the water table electrolytes in the pore fluids undergo oxidation and release electrons which are conducted upwards through the ore body. At the top of the body the released electrons cause reduction of the electrolytes. A circuit thus exists in which current is carried electrolytically in the pore fluids and electronically in the body so that the top of the body acts as a negative terminal. This explains the negative SP anomalies that are invariably observed and their stability as the ore body itself undergoes no chemical reactions and merely serves to transport electrons from depth. As a result of the subsurface currents, potential differences are produced at the surface.

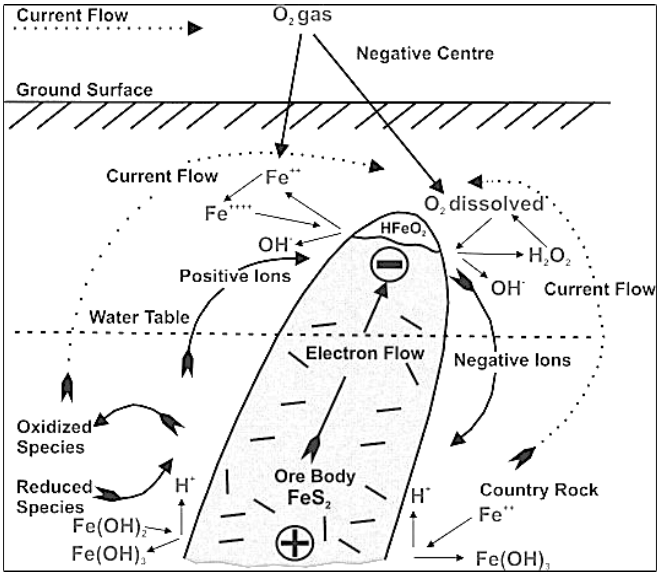

Fig.2.2: The mechanism of self-potential anomalies

2.3 Magnetic Method:

Generally, the aim of a magnetic survey is to investigate subsurface geology on the basis of the anomalies in the earth's magnetic field resulting from the magnetic properties of the underlying rocks. In general, the magnetic content (susceptibility) of rocks is variable depending on the rock type. Commonly causes of magnetic anomalies include dykes, faults and lava flows. In case of geothermal environment, due to high temperatures, the susceptibility decreases. It is not usually possible to identify with certainty the causative bodies of any anomaly from magnetic information alone.

Magnetism is, just like gravity, a potential field. So, it is also possible to transform one potential field to others. Anomalies in the earth's magnetic field are caused by induced or remnant magnetism. Induced magnetic anomalies are the result of secondary magnetization induced in a ferruginous body by the earth's magnetic field. The shape dimensions, and amplitude of an induced magnetic anomaly is a function of the orientation, geometry, size, depth, and magnetic susceptibility of the body as well as the intensity and inclination of the earth's magnetic field in the survey area.

The magnetic method involves the measurement of the earth's magnetic field intensity. At any point on the Earth's surface a freely suspended magnetic needle will assume a position in space in the direction of the ambient geomagnetic field.

This will generally be at an angle to both the vertical and geographic north. A schematic diagram is given below in order to describe the magnetic field vector. The total field vector B has a vertical component Z and a horizontal component H in the direction of magnetic north. The dip of B is the inclination I of the field and the horizontal angle between geographic and magnetic north is the declination D. In the present study total magnetic field has been measured. Measurements are of the horizontal or vertical component or horizontal gradient of the magnetic field.

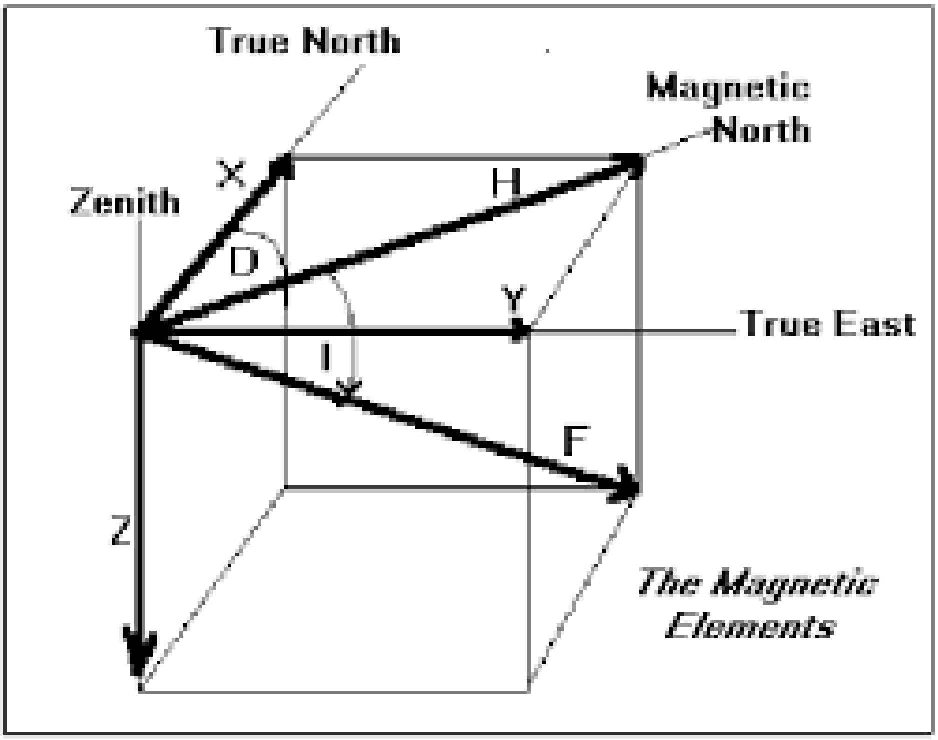

Fig.2.3: Schematic diagram magnetic field vector

3.0 <u>GEOPHYSICAL QUANTUM OF WORK</u>:

The scope of work consists of acquisition, processing and interpretation of ground geophysical data across a prospective mineralized area spanning 3.55 square kilometers. The Profile lines were designed and aligned in such a way that it lays across the regional geological strike direction of the targeted potential zones and to be covered with 30 lines km (3 Unit) of IP, SP and magnetic Survey Profile as approved by NMET.

Survey Details:

The 30-line kilometers were divided into two blocks: Block-I (Fig.5.2) having area 1.767 square kilometers near Sakalgunta village and the Block-II (Fig.5.3) having area 1.134 square kilometers near Bangaragunta village which are possible associated with gold mineralization covering of 18.0 and 12.0 line-kilometers respectively.

The lines were kept at 100 meters spacing with 20 meter as station spacing for recording data. The survey consists of Induced Polarization (IP) cum Resistivity, Ground Magnetic, and Self-Potential (SP) methods to detect subsurface anomalies indicative of mineralization. The objective of the Geophysical survey was to delineate gold mineralization and its host rock with other associated mineralized zone in respective blocks.

4.0 FIELD ACTIVITIES:

A base camp was established near Bargur block at Krishnagiri District to facilitate the geophysical survey in both the blocks. The survey team consisted of three to four members (Table 4.) equipped with specialized instruments including the ENVI Pro Magnetometer for magnetic measurements, the IRIS Syscal R2 Resistivity Meter for SP data recording, the Syskal pro 72 Channels for IP-cum-Resistivity measurements and Trimble Juno Handheld GPS unit for precise location tracking/marking. Detailed specifications of this equipment are provided in Table 5. The location Map/Block boundary map, along with its coordinates, is presented in Figure 5.1. and Table 5.1 respectively. To ensure accuracy and minimize disturbances the magnetic base was established outside of the Bargur block boundary area, as specified in Table.

4.1 DURATION OF WORK:

The Geophysical survey was completed within 75 days i.e. from 01-02-2025 to 15-04-2025

4.2 BACK-OFFICE WORK:

- QA/QC of acquired data on day-to-day basis.
- Preliminary processing of data to check for errors/jumps and any repetition if needed.
- Monitoring of covered Line Km and area.

4.3 LIST OF PERSONNEL

The following personnel were involved in the project as given below:

Sr. No.	Name & Designation	Responsibility
1.	G.S. Dhami GM (GS)	Heading the Project, Planning Monitoring, Liasoning, Data processing, interpretation and report writing.
2.	ABBS Rama Krishna Manager (Geophysicist)	Survey design
3.	Rajat Kumar Geophysicist	Data acquisition, Data QA/QC, Data processing, interpretation& report writing
4.	Vikas Kumar (Contingent Geophysicist)	Data acquisition.
5.	Aman Sharma (Young Geophysicist)	Data acquisition.

Table 4.1: List of Personnel

5.0 EXPLORATION PARAMETER

Project Area And Location:

This area forms the northern part of Krishnagiri District of Tamil Nadu. The area is served by a good network of metalled roads. National Highway No.46 (Chennai-Bangalore Road) passes through the southern end of the area. The area is well connected by Krishnagiri-Kuppam road on the west and Bargur-Gurivinayanapalli road on the east. There are also a number of foot-tracks connecting these roads. Bargur is the nearest Bus station and is just 1 km. from the south-eastern corner of the area. The nearest railway station by road is Jolarpettai junction which is about 35 km. from Bargur.Table 5.1: Coordinates of the corner points of the Bargur Block (3.524 Sq.km)

Bargur block falls in Toposheet No. 56 L/6. Kuppam is 20km away from the block. The nearest rail head is Kuppam (20Km), and Jolarpet Junction, which is 25 km. The nearest airport is Bengaluru (143 Km) from Bargur. (Plate No.1).

Co-ordinates of the corner points of the Block-I (Sakalagunta) (1.767 Sq.km) of Bargur Block.				
Block Corner Points	WGS 84 (DD MM SS)		UTM ZONE 44-N	
	Longitude	Latitude	Easting	Northing
A	78.19.26.84140	12.34.03.61312	209233.8	1390805
B	78.20.00.92666	12.34.03.92050	210263.4	1390804
C	78.20.01.51952	12.33.08.01981	210263.9	1389085
D	78.19.27.46609	12.33.07.71316	209235.2	1389086

Co-ordinates of the corner points of the Block-II (Bangaragunta) (1.134 Sq.km.) of Bargur Block.				
Block Corner Points	WGS 84 (DD MM SS)		UTM ZONE 44-N	
	Longitude	Latitude	Easting	Northing
E	78.20.15.11595	12.33.17.71661	210677.6	1389379
F	78.20.14.30924	12.34.16.44481	210671.5	1391185
G	78.20.35.12284	12.34.16.65154	211300.2	1391185
H	78.20.35.93817	12.33.17.92315	211306.6	1389379

Magnetic Base coordinates				
Magnetic Base	Longitude	Latitude	Easting	Northing
	80.32.39.55900	21.59.14.49850	452960	2431498

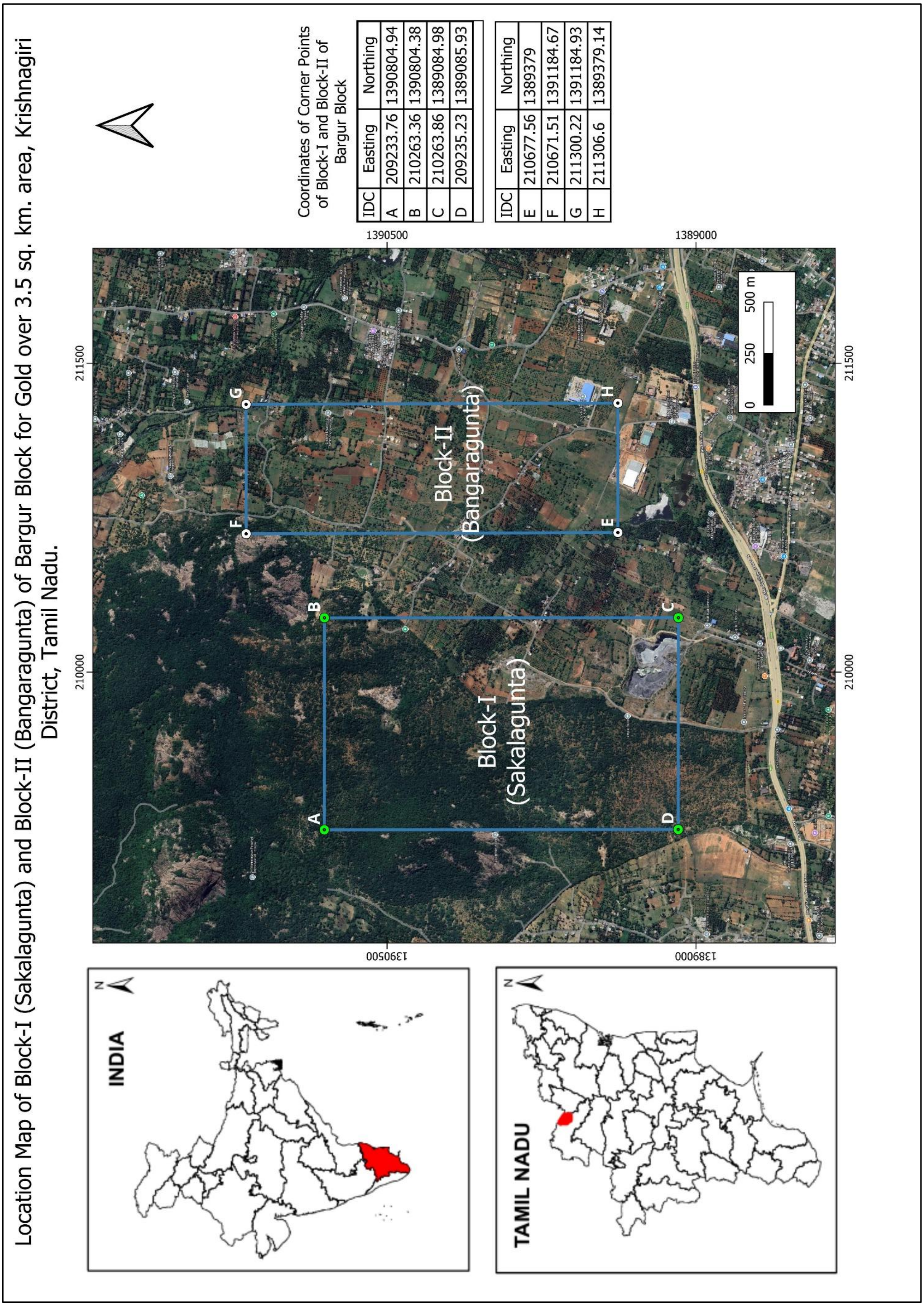

IDC	Easting	Northing
A	209233.76	1390804.94
B	210263.36	1390804.38
C	210263.86	1389084.98
D	209235.23	1389085.93

IDC	Easting	Northing
E	210677.56	1389379
F	210671.51	1391184.67
G	211300.22	1391184.93
H	211306.6	1389379.14

Fig. 5.0.1: Location map of the of Block-I (Sakalagunta) & Block-II (Bangaragunta) of Bargur Block.

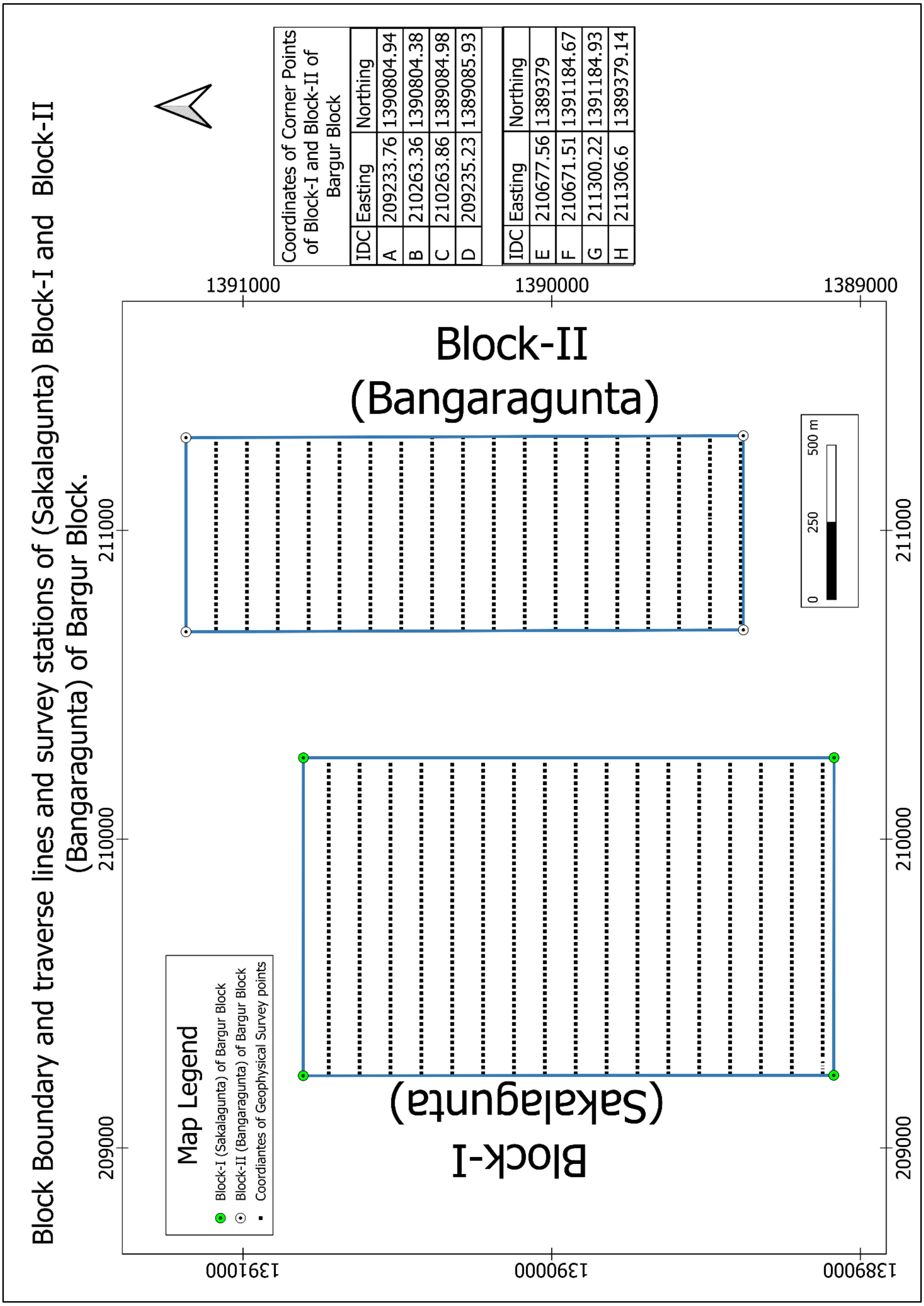

Fig. 5.0.2: Block Boundary and traverse lines and survey stations of Block-I (Sakalagunta) & Block-II (Bangaragunta) of Bargur Block.

Table5.2: Instruments Details

INDUCED POLARIZATION DATA ACQUISITION UNIT	
Type	Multi -Electrode
Make	IRIS (SYSKAL-PRO)
Maximum No of Channel	72
Minimum Channel Interval	10
Sensitivity	1μV/0.2
MAGNETOMETER	
Type	Proton Precision Magnetometer (PPM)
Make	Scintrex (ENVI Pro MAG)
Sensitivity	0.1 nT
Accuracy	+1nT
Range	23000 to 100000 nT
RESISTIVITY METER (SP Measuring Unit)	
Type	SYSCAL R2 Resistivity meter with IP & SP measurements
Make	IRIS Instrument
Input impedance	100 MOhm
Voltage resolution	1 μV/0.2%
Voltage accuracy	0.2%
Automatic compensation of SP	-5V to +5V
SURVEYING	
Type	DGPS
Model	Trimble

5.1 Survey Design and Field Data Acquisition:

The survey stations were fixed in the grid pattern with line interval of 100m and station spacing as 10 m using DGPS and demarcated locations by putting pegs with marked line and station number.

5.2 Magnetic Method:

The survey was designed in a grid pattern with a line interval of 100 meters and a station spacing of 20 meters, with positions marked using Hand held DGPS. Survey locations were meticulously demarcated by placing pegs, each indicating the corresponding line and station number. The layout map of the traverse lines and observation stations is shown in Fig. 4.

The Magnetic data was recorded at every station with starting and ending at the base station on routine basis. The survey was meticulously designed to detect subtle changes in the magnetic field, which could indicate the presence of geological features such as shear zones, faults, and mineralized bodies.

5.3 IP Survey Design:

An induced polarization (IP) survey is conducted using various electrode arrangements, typically involving four electrodes: two current electrodes (C1 and C2) and two potential electrodes (P1 and P2). The choice of electrode configuration depends on the specific objectives of the survey. Different arrangements can provide different responses based on geological conditions. For instance, to map lateral changes in geological structures, the Dipole-Dipole and Werner arrays are often more effective. In this case, the Dipole-Dipole array, as illustrated in Figure 4.2.1, has been employed for the Block survey, with the preplanned survey block shown in Figure 4.1.1.

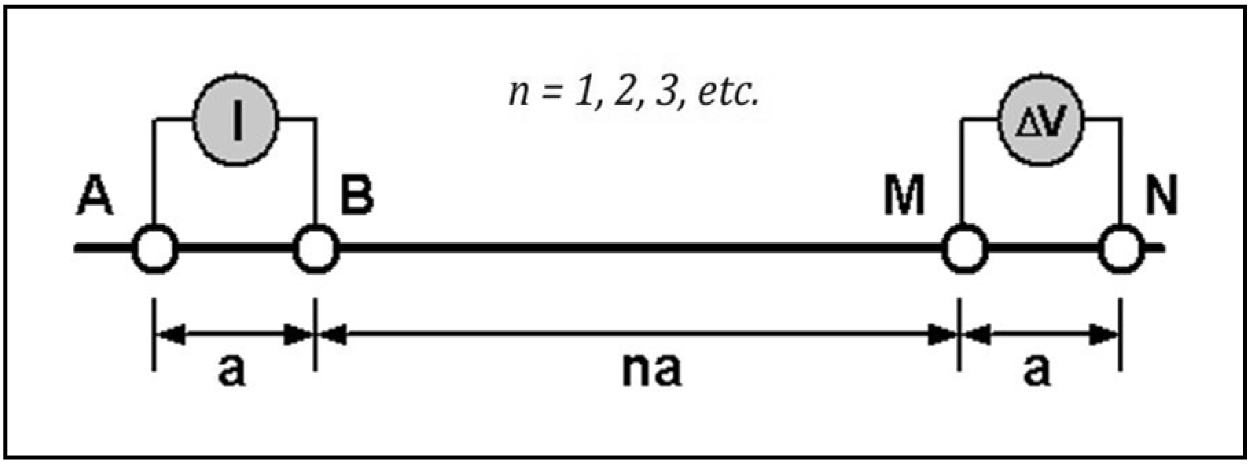

Fig. 5.3.1.: Dipole – Dipole Configuration.

In the current field survey, a total of 36 channels were used for subsurface imaging, with an electrode spacing of 20 meters and a maximum array length of 720 meters. The multi-electrode channel system automatically selects various combinations of current (C1 and C2) and potential (P1 and P2) electrodes from the 36 available electrodes, enhancing the efficiency of subsurface imaging within an optimal timeframe. Throughout the survey block, a cumulative total of 31-line kilometers of profile data were recorded. A graphical representation of the multi-electrode system is provided for better illustration.

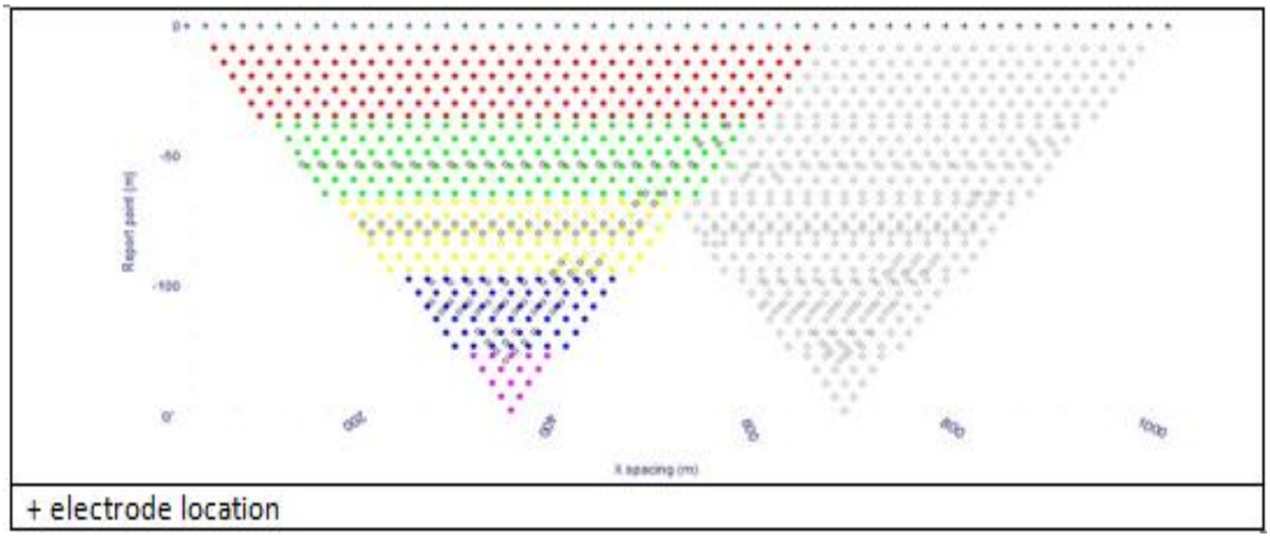

Fig. 5.3.2: Data acquisition pattern in subsurface for roll along profiles.

5.4 SP Survey Design:

The SP survey was carried out using non-polarizing electrodes and a high-impedance voltmeter, along with an SYSCAL R2 system. The recording was done in a grid pattern, with a station spacing of 20 meters and line spacing of 100 meters. A total of 30 LKM was covered.

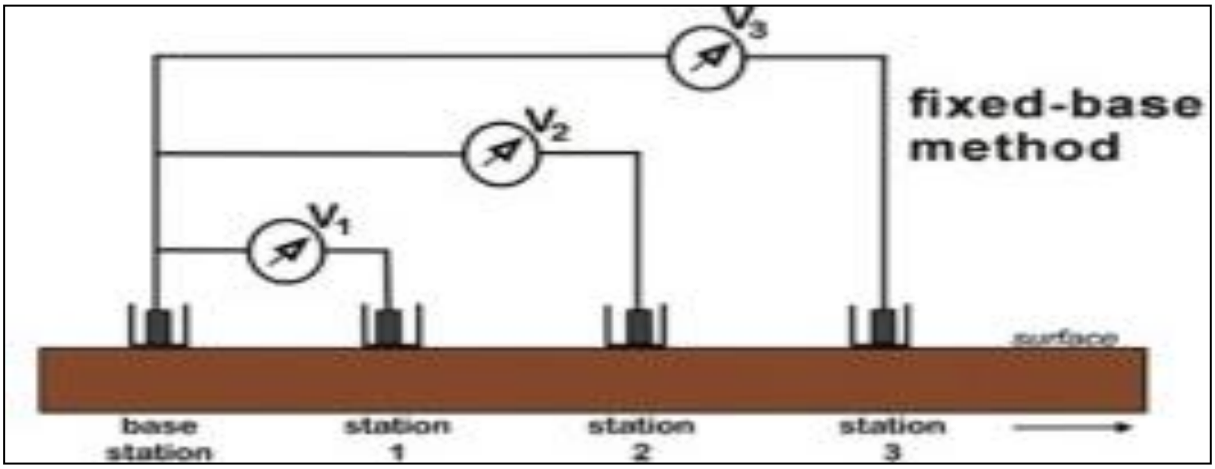

Fig. 5.4: Fixed Base SP Method Survey Configuration

6.0 Data Reduction and Processing.

6.1 Magnetic Survey:

Recorded magnetic data was corrected for diurnal variation of the geomagnetic field with respect to the base station where data was recorded at the start and end of every day field work. IGRF correction of model 2020 was applied on the data set to overcome the large-scale structure of the Earth's main magnetic field and its secular variation. The data was processed using Geosoft Oasis Montaj software and the below listed magnetic anomaly maps have been generated.

6.1.1 Maps for Block-I (Sakalagunta) of Bargur Block.

- Total Magnetic Intensity (TMI) Map. (Fig.6.1.1.1)
- Magnetic Anomaly (MA) Map of Block-I (Sakalagunta) of Bargur Block. (Fig.6.1.1.2)
- Reduced to Pole (RTP) Map of (TMI) of Block-I (Sakalagunta) of Bargur Block. (Fig.6.1.1.3)
- Upward Continuation Map of Magnetic Anomaly at 100 m of Block-I (Sakalagunta) of Bargur Block. (Fig.6.1.1.4)
- Residual Anomaly Map of Magnetic Anomaly at 100 m of Block-I (Sakalagunta) of Bargur Block. (Fig.6.1.1.5)
- Analytical Signal Analysis (ASA) Map of Block-I (Sakalagunta) of Bargur Block. (Fig.6.1.1.6)
- Radially Average Power Spectrum of Block-I (Sakalagunta) of Bargur Block. (Fig.6.1.1.7)
- Integrated Interpretation Map showing Proposed Borehole inferred location at Bargur Block-I (Sakalagunta) of Bargur Block. (Fig.6.1.1.8)

After applying diurnal corrections, the recorded magnetic data showed variation of 980 nT with the highest total magnetic intensity value of 41991.9 nT and minimum of 41011.7 nT was observed in TMI map (Fig. 6.1.1.1). While the magnetic anomaly with respect to IGRF shows a minimum of -846.0 nT and maximum of 122.6 nT in Magnetic Anomaly Map (Fig. 6.1.1.2).

6.1.2 Maps for Block-II (Bangaragunta) of Bargur Block.

- Total Magnetic Intensity (TMI) Map. (Fig.6.1.2.1)
- Magnetic Anomaly (MA) Map of Block-II (Bangaragunta) of Bargur Block. (Fig.6.1.2.2)
- Reduced to Pole (RTP) Map of (TMI) of Block-II (Bangaragunta) of Bargur Block. (Fig.6.1.2.3)
- Upward Continuation Map of Magnetic Anomaly at 100 m of Block-II (Bangaragunta) of Bargur Block. (Fig.6.1.2.4)
- Residual Anomaly Map of Magnetic Anomaly at 100 m of Block-II (Bangaragunta) of Bargur Block. (Fig.6.1.2.5)
- Analytical Signal Analysis (ASA) Map of Block-II (Bangaragunta) of Bargur Block. (Fig.6.1.2.6)
- Radially Average Power Spectrum of Block-II (Bangaragunta) of Bargur Block. (Fig.6.1.2.7)
- Integrated Interpretation Map showing Proposed Borehole inferred location at Bargur Block-II (Bangaragunta) of Bargur Block. (Fig.6.1.2.8)

After applying diurnal corrections, the recorded magnetic data showed variation of 1627nT with the highest total magnetic intensity value of 42115.6 nT and minimum of 40487.7 nT was observed in TMI map (Fig. 6.1.2.1). While the magnetic anomaly with respect to IGRF shows a minimum of -247.2 nT and maximum of 1380.4 nT in Magnetic Anomaly Map (Fig. 6.1.2.2).

6.2 Induced Polarization (IP) And Resistivity Profiles:

The resistivity data were checked station-wise to remove any near surface effect prevailing in the data. The pseudo-depth data were inverted using the RES2DINV software to bring out the subsurface resistivity and chargeability distribution. The inverted sections for recorded IP and

Resistivity data are processed in following order to obtain subsurface 2D models: -

1. Geo-referencing.
2. Edit/Mute (Noises).
3. Generate 2D models of subsurface with the help of IP and Resistivity data (Fig. 6.2.1.1 to Fig. 6.2.1.4) of Block-I (Sakalagunta) of Bargur Block.
4. Generate 2 D models of subsurface with the help of IP and Resistivity data (Fig. 6.2.2.1 to Fig. 6.2.2.6) of Block-II (Bangaragunta) of Bargur Block.

6.3 Self-Potential (SP) Profiles:

The SP data was processed using Geosoft Oasis montaj software.

6.3.1 Block-I (Sakalagunta) of Bargur Block

Total SP anomaly Map (Fig.6.3.1.1) have been generated from the SP data. Total variation in SP value was observed with the highest value of 180.09 mV and mV -168.10 mV as lowest.

1. Total SP anomaly Map of Block-I (Sakalagunta) of Bargur Block. (Fig.6.3.1.1)

6.3.2 Block-II (Bangaragunta) of Bargur Block.

Total SP anomaly Map (Fig.6.3.2.1) have been generated from the SP data. Total variation in SP value was observed with the highest value of 59.4 mV and mV -125.3 mV as lowest.

1. Total SP anomaly Map of Block-II (Bangaragunta) of Bargur Block. (Fig.6.3.2.1)

7.0 RESULTS OF GEOPHYSICAL SURVEY

7.1 Magnetic:

7.1.1 Block-I (Sakalagunta) of Bargur Block

A total variation of **≈ 980 nT** is observed in the TMI data, with the maximum value recorded at **41,991.1 nT** and the minimum at **41,011.7 nT** (Figure 6.1.1.1). Similarly, the Magnetic Anomaly (MA) exhibits a total variation of near 980 nT, with the highest value recorded at 122.6 nT and the lowest at -846.0 nT, as illustrated in Figure 6.1.1.2.

The magnetic survey reveals a significant variation (≈ 980 nT) in both the total magnetic field and magnetic anomalies, with a distinct dominance of N-S oriented structural control, especially in the northern portion of the area, accompanied by secondary E-W trends. The pattern of highs and lows suggests a varied subsurface with magnetically strong lithologies and shallow sources in some zones, and deeper or less magnetic material in others further suggesting structural influences.

7.1.2 Block-II (Bangaragunta) of Bargur Block.

A total variation of 1627 nT in the Total Magnetic Intensity (TMI) was observed, with the highest value recorded at 42115.6 nT and the lowest at 40487.7nT. Similarly, the Magnetic Anomaly (MA) showed a total variation of 1627 nT, with a maximum value of 1380.4 nT and a minimum of -247.2 nT, as illustrated in Figures 6.1.2.1 and 6.1.2.2, respectively.

The Total Magnetic Intensity (TMI) map of Block-II reveals significant magnetic anomalies that suggest notable variations in the subsurface geology. The TMI values range from approximately **40,487.7 nT to 42,115.6 nT**, indicating zones of high and low magnetic susceptibilities. The central region of the block shows elevated magnetic values (pink to red zones), which may correspond to magnetite-rich formations or igneous intrusions. The lower magnetic intensity zones (deep blue to green) observed in the southern and northern parts may represent less magnetic lithologies such as sedimentary rocks or zones of deep weathering. The linear trends in magnetic variation suggest the presence of faulting or folding, possibly influencing the emplacement of magnetic bodies.

7.2 Reduced To Pole (RTP):

Because of the dipolar nature of geomagnetic field, the magnetic sources observed anywhere except magnetic poles are asymmetric, this feature makes the interpretation of magnetic data difficult. The reduced to pole (RTP) technique is implemented over the Magnetic anomaly grid in order to convert magnetic anomaly to symmetrical shape so that the angle of inclination is 90 degree and declination is zero and hence, the effect of dipoles were eliminated.

Block-I (Sakalagunta) of Bargur Block

The Reduction to the Pole (RTP) transformation of the magnetic anomaly map for Block-I was generated to enhance structural trends and highlight anomalous features.

The Reduction to Pole (RTP) processing has made the magnetic anomalies more symmetric, reducing the asymmetry caused by the oblique geomagnetic field. Despite the RTP correction, a **continuous structural trend** is *not* clearly visible in Block-I. The anomalies are patchy, somewhat isolated and do not form a single coherent linear feature.

Although the RTP processing improved the clarity of magnetic anomalies and partially aligned them in the N–S direction, thus reducing the asymmetric effects of magnetic sources, no continuous structural trend is distinctly visible in the RTP map. This suggests that the magnetic sources may be discontinuous or structurally complex in nature, as shown in Fig. 6.1.1.3. For exploration, this means that one must treat anomaly zones individually, rather than assuming a continuous target. The highest priority should be given to well-defined, high amplitude anomalies, especially where they coincide with structural intersections or favourable lithology.

Block-II (Bangaragunta) of Bargur Block.

The Reduced-To-Pole (RTP) magnetic anomaly map of Block-II offers a clearer picture of the magnetic source geometry by repositioning anomalies directly over their causative bodies. The map displays magnetic intensity values ranging from approximately **48.4 to 390.0 nT**, with several high-amplitude anomalies (shown in pink to red tones) concentrated in the central and southern regions.

These high magnetic zones likely indicate the presence of strongly magnetized lithologies, such as mafic or ultramafic intrusions, which may host economic mineralization. The magnetic lows (blue to green zones), particularly in the northern and southwestern parts of the block, suggest either non-magnetic sedimentary cover or deeper basement structures. The well-defined anomaly shapes and gradients hint at structural features like faults or contacts between contrasting lithologies as illustrated in Fig. 6.1.2.3.

7.3 Residual Magnetic Anomaly:

Block-I (Sakalagunta) of Bargur Block

The Residual Magnetic Anomaly Map (Fig. 6.1.1.5) was generated by subtracting the 100 m Upward Continuation Map (Fig. 6.1.1.4) from the Magnetic Anomaly Map (Fig. 6.1.1.2) using the "Grid Math" function in Geosoft Oasis Montaj software. This residual map effectively highlights local geological features and structures by minimizing the influence of broader regional trends.

The residual anomaly map for Block I reveals that beneath the regional / deeper magnetic background, there are many local magnetic features of interest. These local features suggest significant lithologic variation and shallow magnetic sources. However, the lack of a continuous structural trend even at residual scale suggests that the subsurface geology is complex, with perhaps many small bodies rather than large cohesive ones.

For exploration, the localized, high residual anomalies should be focused on—especially where they align with inferred structural features or where geology indicates favorable rock types. Such anomalies are likely to yield more immediate geological information or targets than relying on the broader, less detailed trends (Fig. 6.1.1.5).

Block-II (Bangaragunta) of Bargur Block.

The Residual Magnetic Anomaly Map (Fig. 6.1.2.5) was generated by subtracting the 100 m Upward Continuation Map (Fig. 6.1.2.4) from the Magnetic Anomaly Map (Fig. 6.1.2.2) using the “Grid Math” function in Geosoft Oasis Montaj software. This residual map effectively highlights local geological features and structures by minimizing the influence of regional magnetic trends.

In the residual anomaly map, the magnetic anomaly previously observed in the northwestern part of the study area has disappeared. This suggests that the anomaly in that region was primarily associated with regional geological influences. In contrast, the anomaly observed in the southeastern part of the block, trending in a N-S direction, remains prominent. This anomaly is likely associated with shear facies in the study area and is more distinctly represented as a residual feature.

Overall, the residual magnetic anomaly map enhances the visibility of smaller, localized anomalies that were previously obscured by strong regional disturbances in the original magnetic anomaly map.

7.4 Analytic Signal Analysis Map:

Block-I (Sakalagunta) of Bargur Block

The Analytical Signal analysis, also known as the Total Gradient method, is a reliable technique for delineating the edges and lithological boundaries of magnetic source bodies. A key strength of this method is its relative independence from the magnetic field orientation and remanent magnetization.

The Analytical Signal Amplitude Map (Fig. 6.1.1.6) of the area reveals high-intensity signal amplitudes along geological contacts and shallow magnetic bodies, indicating potential lithological boundaries. However, no continuous trend was observed across the block, suggesting that the magnetic sources are more localized and discontinuous in nature.

Block-II (Bangaragunta) of Bargur Block.

The Analytical Signal analysis, also referred to as the Total Gradient method, is an effective tool for identifying the edges and lithological boundaries of magnetic source bodies. Its primary advantage lies in the fact that the shape of the analytical signal is nearly independent of the magnetic field orientation and remanent magnetization.

The Analytical Signal Amplitude Map (Fig. 6.1.2.6) of the study area displays high-intensity signal amplitudes along geological contacts and over shallow anomalous sources, helping to infer subsurface lithological boundaries. Contour lines, marked in white, clearly delineate the boundaries of the causative magnetic bodies.

7.5 Radially Average Power Spectrum:

The Radially Averaged Power Spectrum (RAPS) plots for Block-I and Block-II, as shown in Fig. 6.1.1.7 and Fig. 6.1.2.7 respectively, indicate that the majority of the magnetic anomaly features and their causative bodies lie within a depth range of approximately **100 to 500 meters**. This depth estimation provides valuable insight into the subsurface geological structures and supports the interpretation of near-surface and intermediate-depth magnetic sources across both blocks.

7.6 Induced Polarization (IP) Profiles:

The Resistivity cum IP (Induced Polarization) response in the survey area is characterized by low resistivity and high chargeability values, which are typically associated with Sulphide and Oxides minerals and alteration and shear zones. The combination of low resistivity and high chargeability suggests the presence of mineralized zones, likely containing sulfides or other conductive minerals, within these altered geological formations.

7.7 IP Response:

Block-I (Sakalagunta) of Bargur Block

The Induced Polarization (IP) survey data reveal significantly low resistivity values and high chargeability values exceeding 40 mV/V along the survey lines. This combination is indicative of the presence of conductive formation zones, which may correspond to gold, copper, and associated mineralization.

A continuous trend is observed from Line 4 to Line 16, after which the trend becomes discontinuous. The dark red zones, corresponding to high chargeability values, and the dark blue zones, reflecting low resistivity, highlight anomalous areas that extend up to 135 meters in depth, as shown in the IP anomaly profiles.

In areas with closely spaced data points, the geophysical anomalies are better defined. Notably, the central part of the block shows overlapping low resistivity and high chargeability values, suggesting continuous mineralization extending to the full investigated depth of 120 meters.

These anomalous zones are illustrated in Figures 6.2.1.1 to 6.2.1.4

Block-II (Bangaragunta) of Bargur Block.

The Resistivity values along the IP lines are significantly low, while the chargeability values are elevated, exceeding 40 mV/V. This combination of low resistivity and high chargeability suggests the presence of conductive formation zones, which may correspond to gold mineralization within the surveyed area.

Although no consistent trend is observed across all lines, areas showing localized zones of low resistivity and high chargeability may indicate potential mineralization. These zones generally align in a north-south (N-S) direction across the survey area.

Notably, the resistivity and chargeability anomalies in the central part of the block suggest continuous mineralization extending to a depth of 120 meters (the full depth of the survey investigation).

These anomalous zones are shown in Figures 6.2.2.1 to 6.2.2.6.

7.8 SELF-POTENTIAL (SP) SURVEY:

Block-I (Sakalagunta) of Bargur Block

The total SP anomalies along each traverse have been generated from the SP data. The total variation of the SP anomaly observed was 348 mV, with the highest value recorded at 180 mV and the lowest at -168 mV. The SP data reveal significant structural disturbances in the area, as shown in Figures 6.3.1.1 and 6.3.1.2.

The SP data correlate well with the IP, resistivity, and magnetic data, suggesting that the electro-kinetic potential observed in the shear zones is likely due to sulphide mineralization. The low SP values align closely with areas identified by the IP and other data sets, reinforcing the interpretation of the shear zone's role in the mineralization process.

Block-II (Bangaragunta) of Bargur Block.

The Spontaneous Potential (SP) survey results over Block-II reveal a significant variation in natural electric potentials, with values ranging from **+59.4 mV to -125.3 mV**, amounting to a total variation of **184.7 mV**. These anomalies, as illustrated in **Figures 6.3.2.1 and 6.3.2.2**, are indicative of **subsurface electro-kinetic processes** and are typically associated with **sulfide mineralization**. The SP anomalies display a **north-south (N-S) trend**, correlating strongly with chargeability and resistivity anomalies from the **IP survey**, as well as with the magnetic highs and structural features delineated in the **TMI, RTP, and ASA maps**.

The **negative SP anomalies**, particularly prominent in the central and southern portions of Block-II, coincide spatially with zones of **high IP chargeability** and **low resistivity**, reinforcing the interpretation of **disseminated or vein-hosted sulfide mineralization**.

8.0 CONCLUSION AND RECOMMENDATIONS

8.1.0 Block-I (Sakalagunta) of Bargur Block

The integrated geophysical survey as approved by NMET has been conducted in the Sakalagunta and Bangaragunta block of Bargur Block by adopting IP cum resistivity, SP and Magnetic methods. The objective of the survey was to find out the potential zones for base metals comprising Gold and other associated mineralisation. The effectiveness of these methods along with its limitation depends upon the physical properties contrast of the target and surroundings. To demarcating the zones of interest and their contacts spatial filtering technique like Upward continuation, Horizontal derivatives and analytical signal analysis etc. were applied on magnetic data to enhance the outcomes.

The area of possible mineralization has also been marked in IP and apparent Resistivity sections and has plotted over profile. In order to obtain source depth information, radially averaged power spectrum and analytical signal analysis maps of Magnetic anomaly etc. has been generated and depth of the anomalous zones were found ranging from 80m to 140m in different segments of the block.

8.1.1 Block-I (Sakalagunta) of Bargur Block:

Sakalagunta Block exhibit moderate magnetic complexity with several discrete anomalous zones rather than a single, coherent structural body. The Total Magnetic Intensity (TMI) and Magnetic Anomaly (MA) maps show a variation of ~980 nT, with both high positive and negative anomalies, indicating contrasts in both magnetic mineral content and source depth. The Reduction to Pole (RTP) transformation improves symmetry of these anomalies but still not reveal a continuous N–S-oriented structure suggesting that magnetic sources are discontinuous. Based on these integrated geophysical results, three boreholes have been proposed over the Analytical Signal (Magnetic) maps targeting the identified alteration and shear zones.

For the phase-1: Three borehole locations are proposed for further confirmation or exploration.

Below table is showing the inferred location of the borehole.

Table 6- Proposed inferred Borehole Locations for Block-I (Sakalagunta) of Bargur Block.

BHID	Line	IP-Station	Depth	Easting	Northing
1	11	515	120	209761.3	1390122
2	9	560	98	209801.3	1389922
3	14	500	95	209741.3	1390422

8.1.2. Block-II (Bangaragunta) of Bargur Block.:

In Block-Bangaragunta, two boreholes have been proposed within a low to moderate magnetic zone. The locations are further supported by IP-resistivity data, which reveal low resistivity and high chargeability—geophysical signatures indicative of sulphide mineralisation.

Two boreholes are proposed along **Line 29** and **Line 32**, all of which fall within a **low to moderate magnetic zone**. These zones exhibit **low to moderate resistivity** and **high chargeability**, suggesting a potential association with mineralization. Below table is showing the inferred location of the borehole.

Table-7: Proposed inferred Borehole Locations for Block-II (Bangaragunta) of Bargur Block.

BHID	Line	IP-Station	Depth	Easting	Northing
1	32	240	90	210921.3	1390787
2	29	220	90	210901.3	1390487

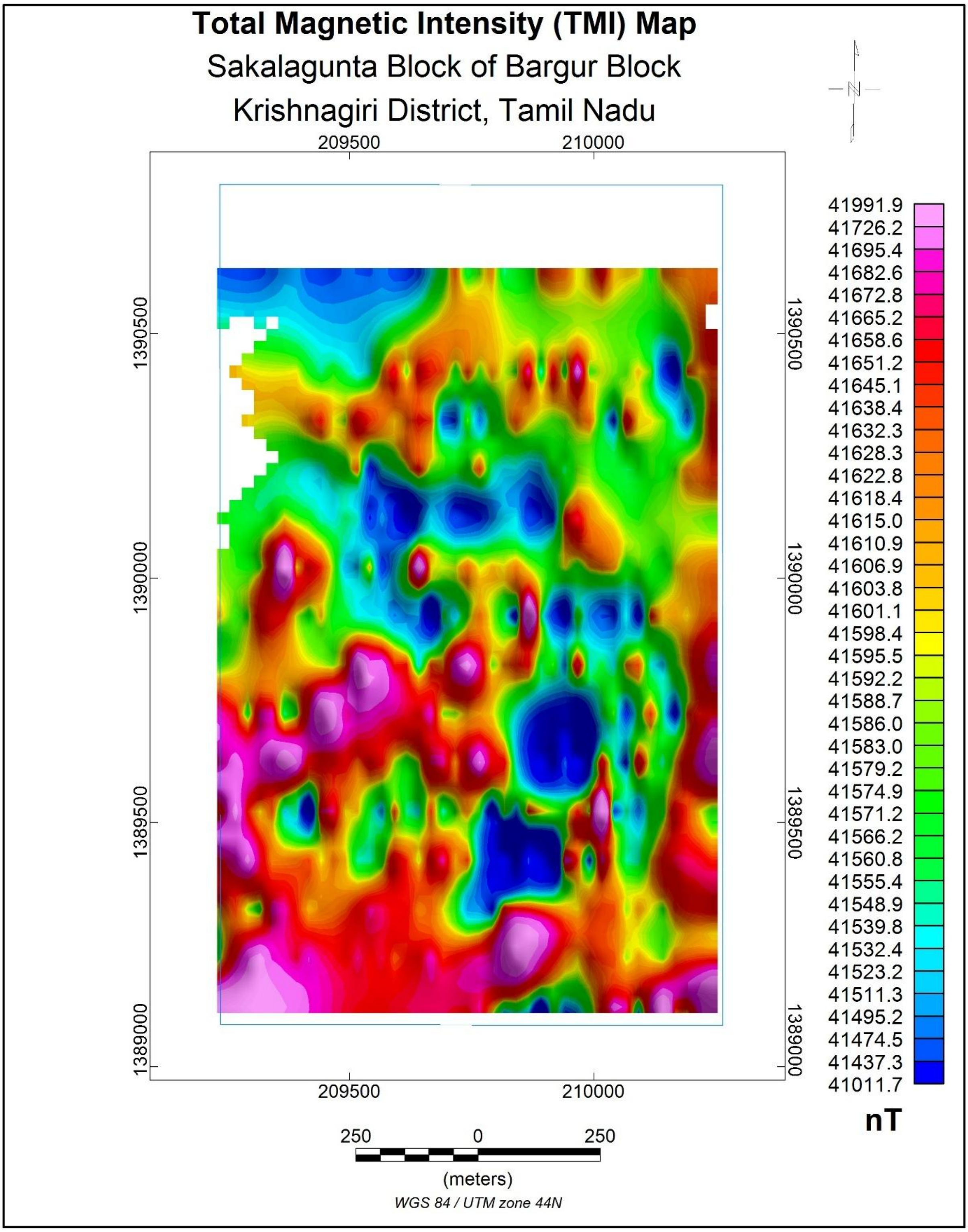

Fig. 6.1.1.1: Total Magnetic Intensity (TMI) Map of Block-I (Sakalagunta) of Bargur Block.

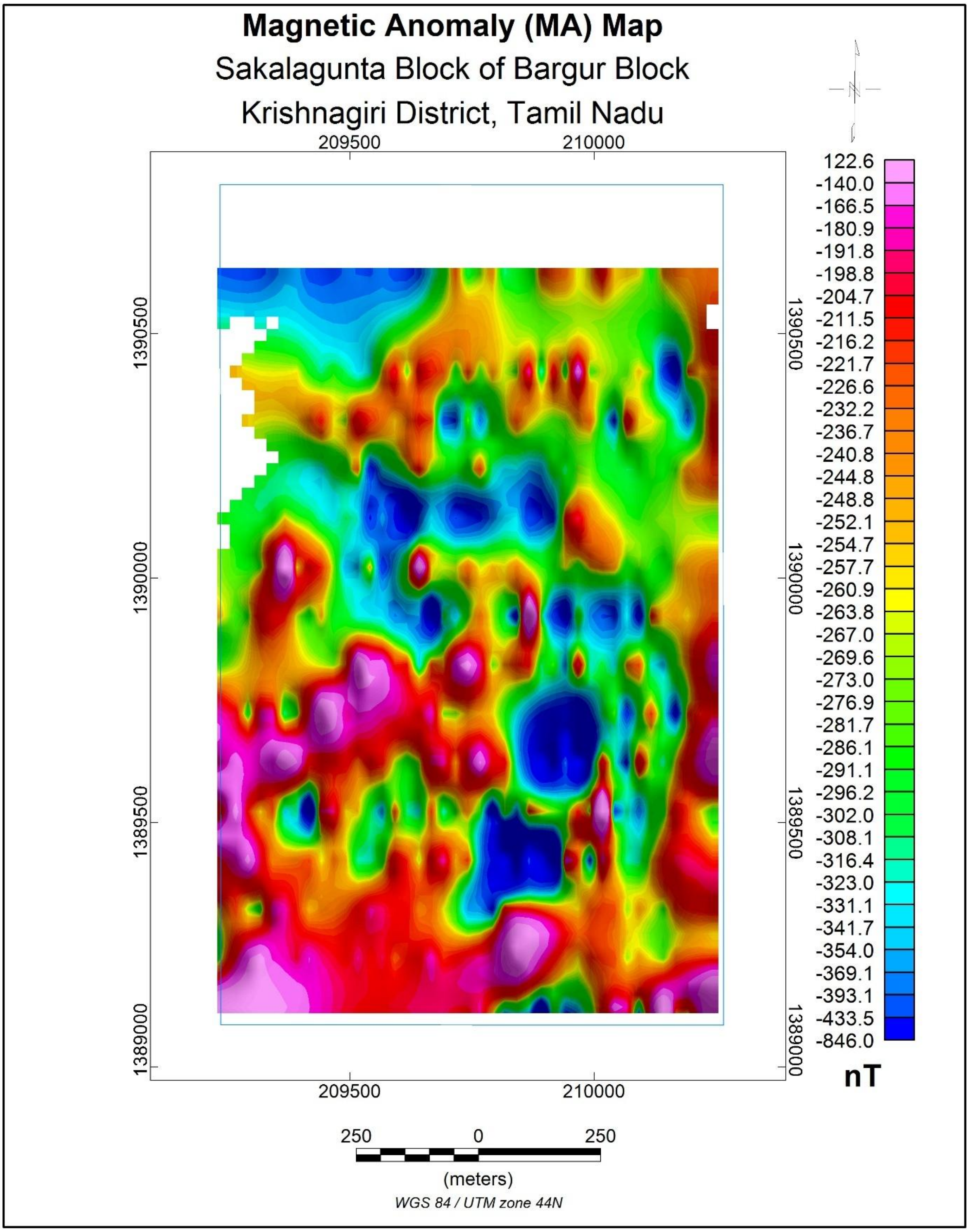

Fig. 6.1.1.2: Magnetic Anomaly (MA) Map of Block-I (Sakalagunta) of Bargur Block.

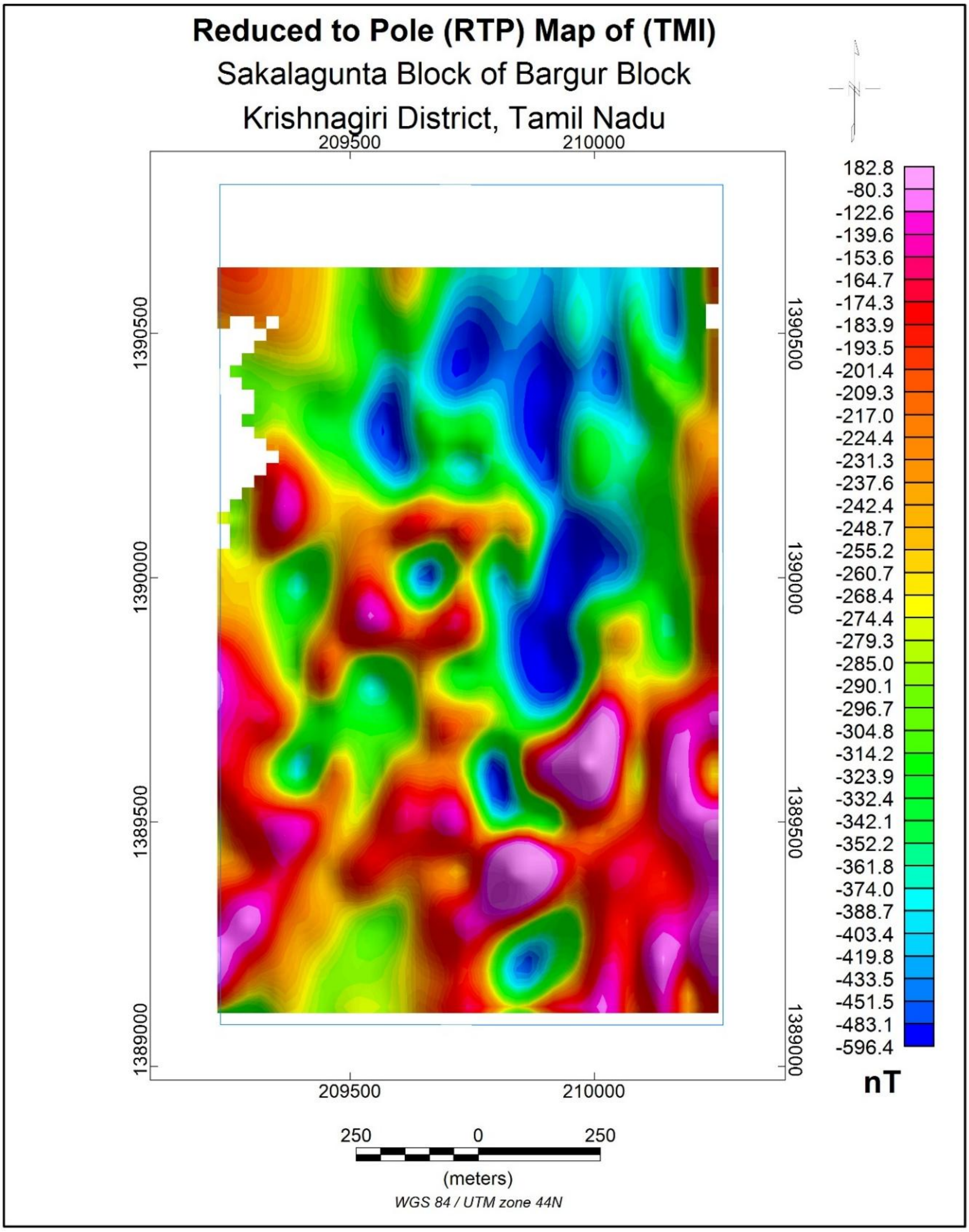

Fig. 6.1.1.3: Reduced to Pole (RTP) Map of (TMI) of Block-I (Sakalagunta) of Bargur Block.

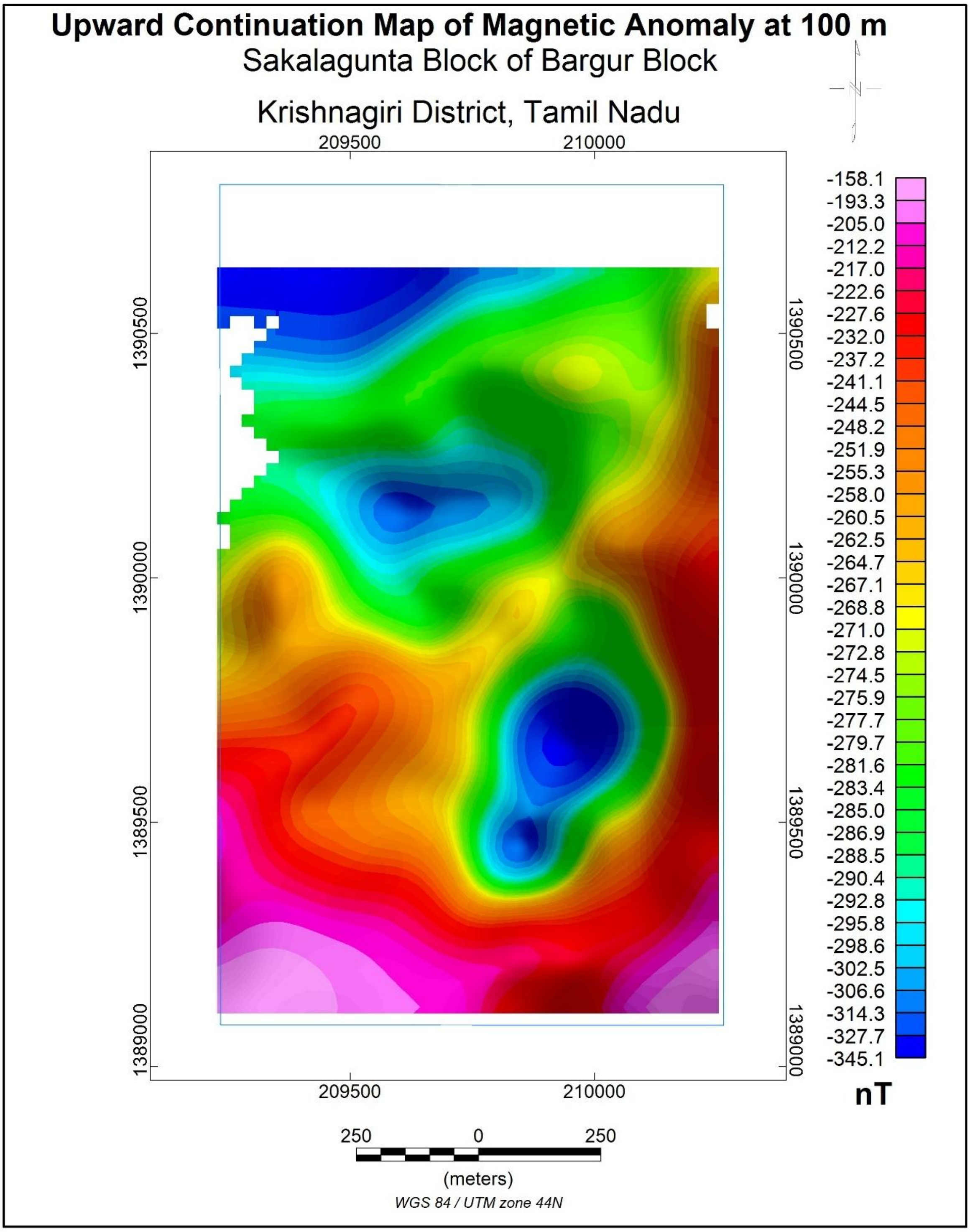

Fig. 6.1.1.4: Upward Continuation Map of Magnetic Anomaly at 100 m of Block-I (Sakalagunta) of Bargur Block.

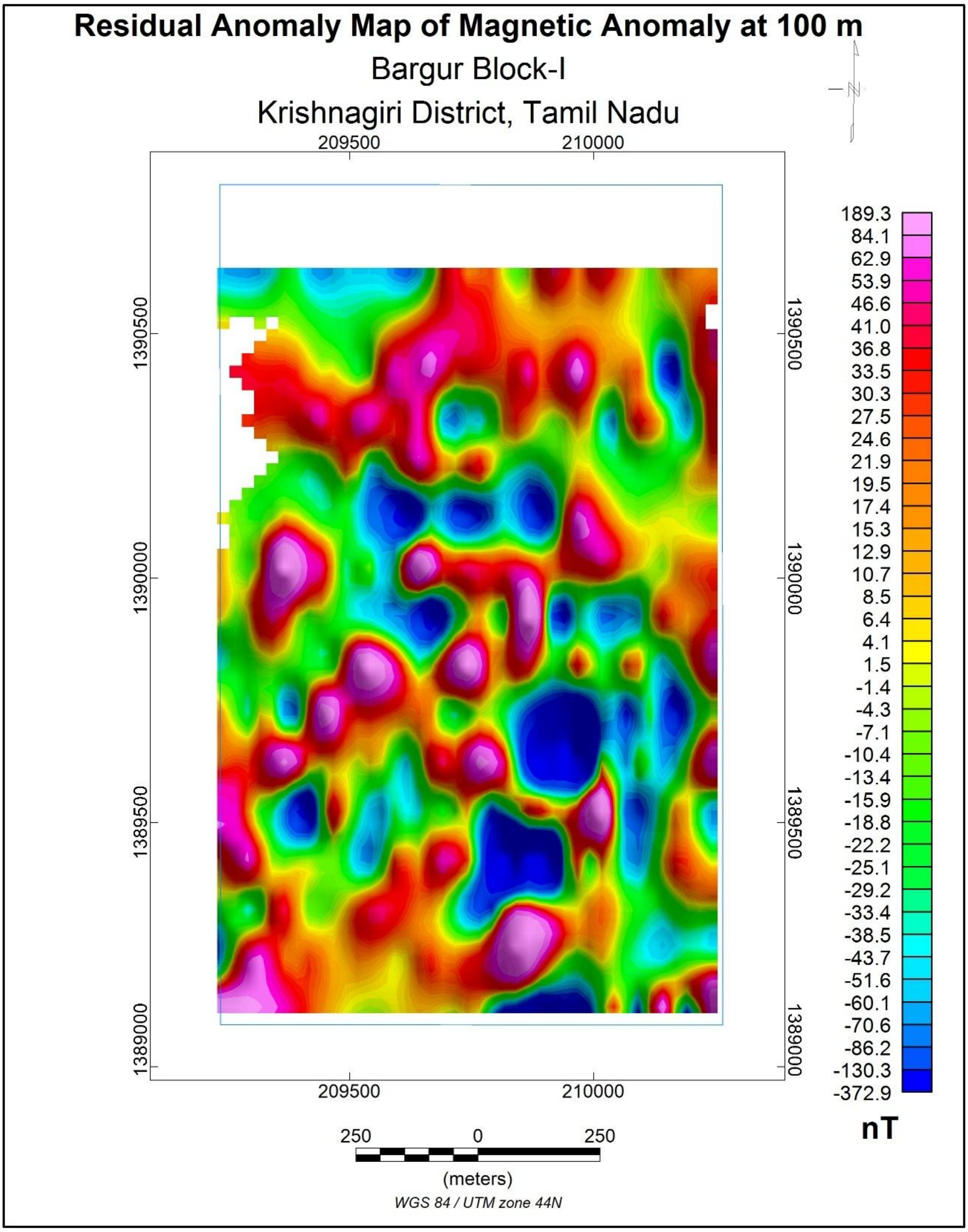

Fig. 6.1.1.5: Residual Anomaly Map of Magnetic Anomaly at 100 m of Block-I (Sakalagunta) of Bargur Block.

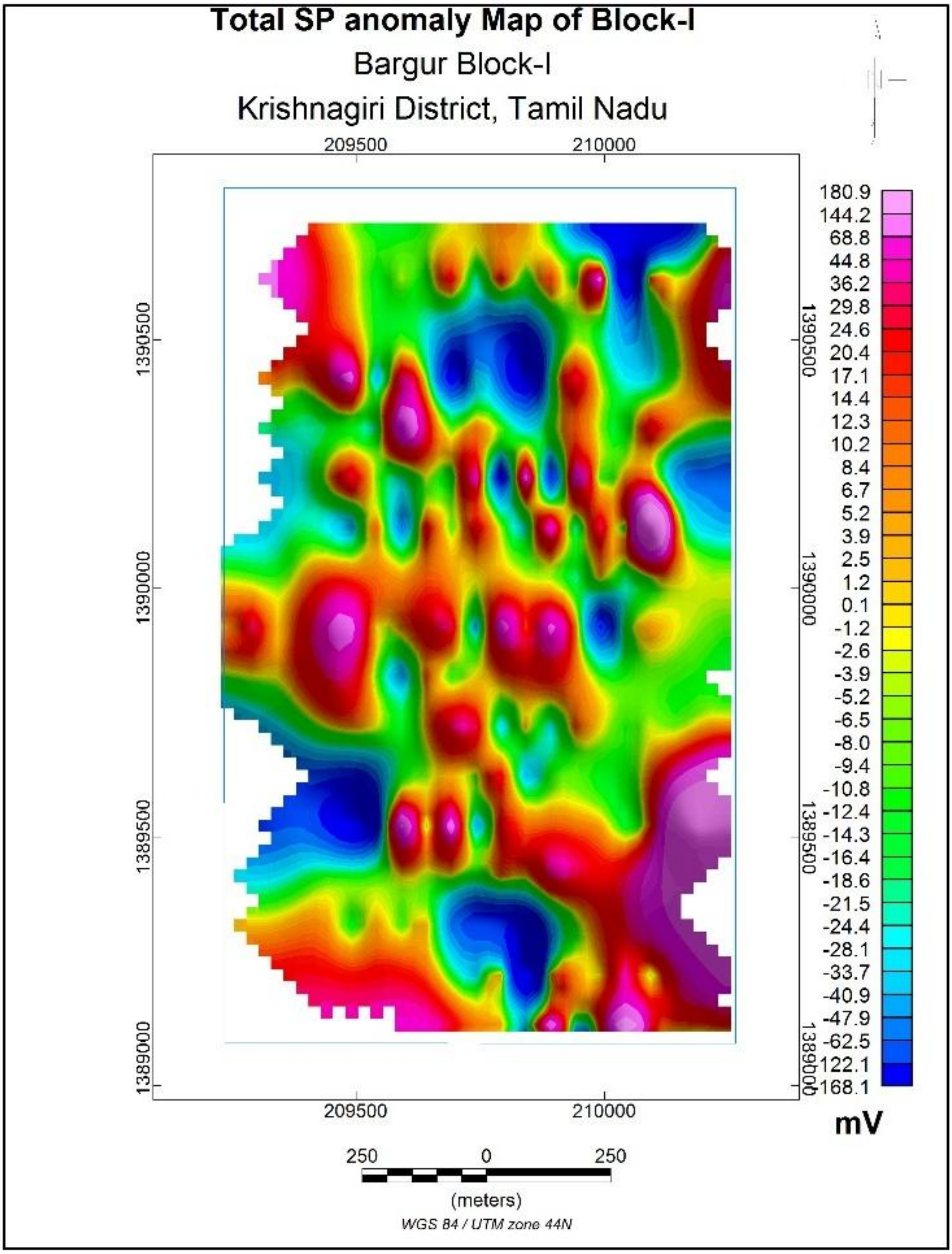

Fig. 6.1.1.6: Analytical Signal Analysis (ASA) Map of Block-I (Sakalagunta) of Bargur Block.

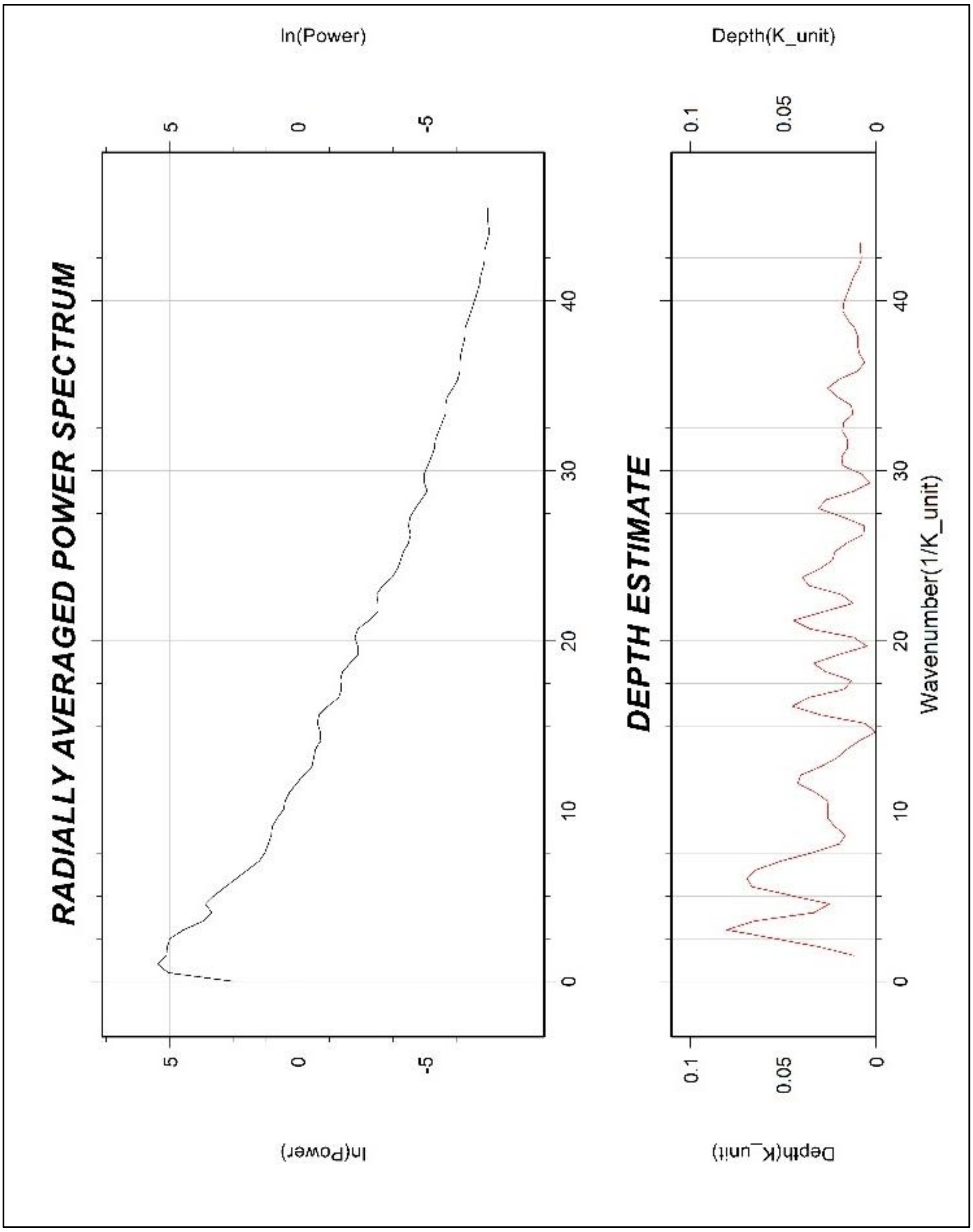

Fig. 6.1.1.7: Radially Average Power Spectrum of Block-I (Sakalagunta) of Bargur Block.

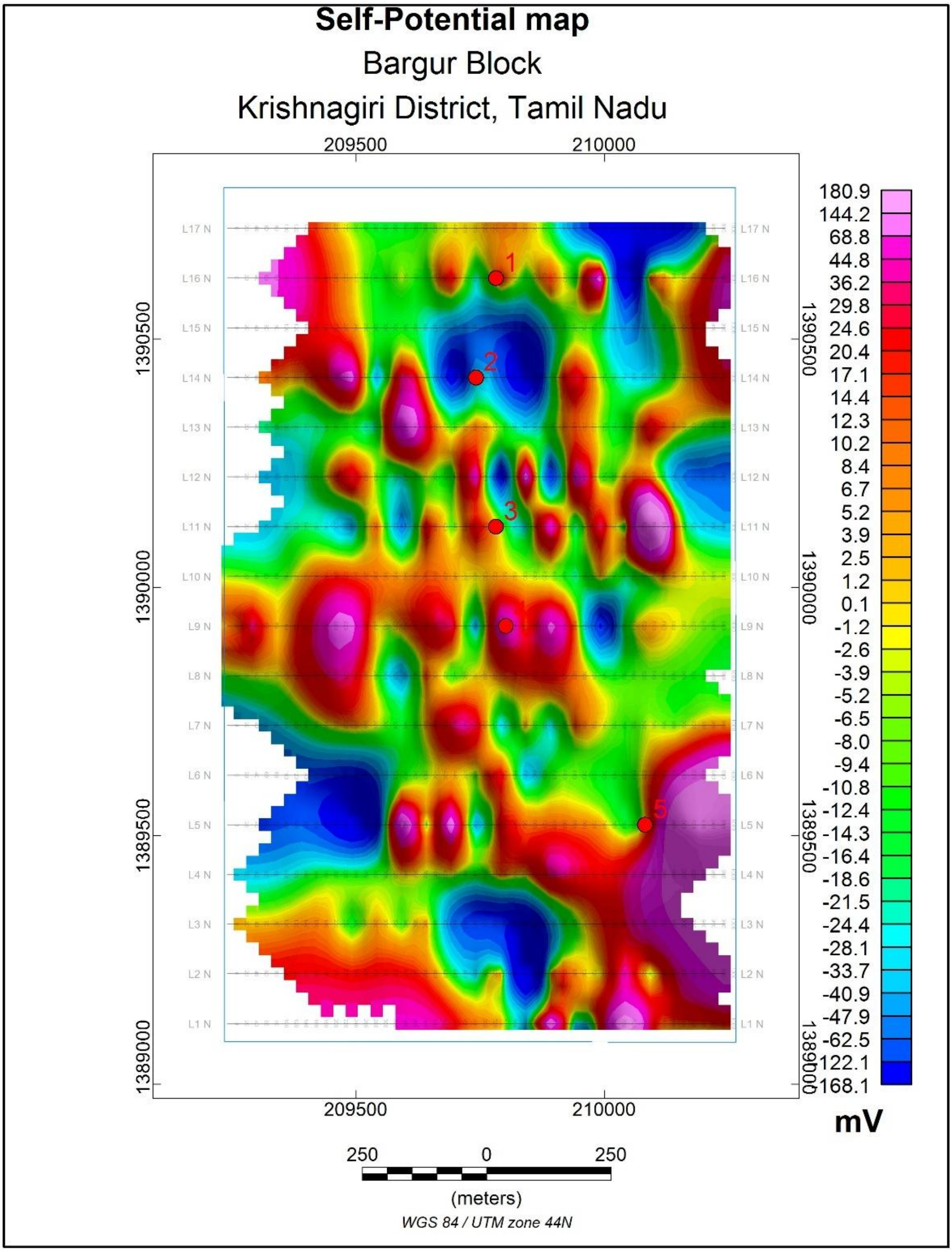

Fig. 6.3.1.1: Total SP anomaly Map of Block-I (Sakalagunta) of Bargur Block.

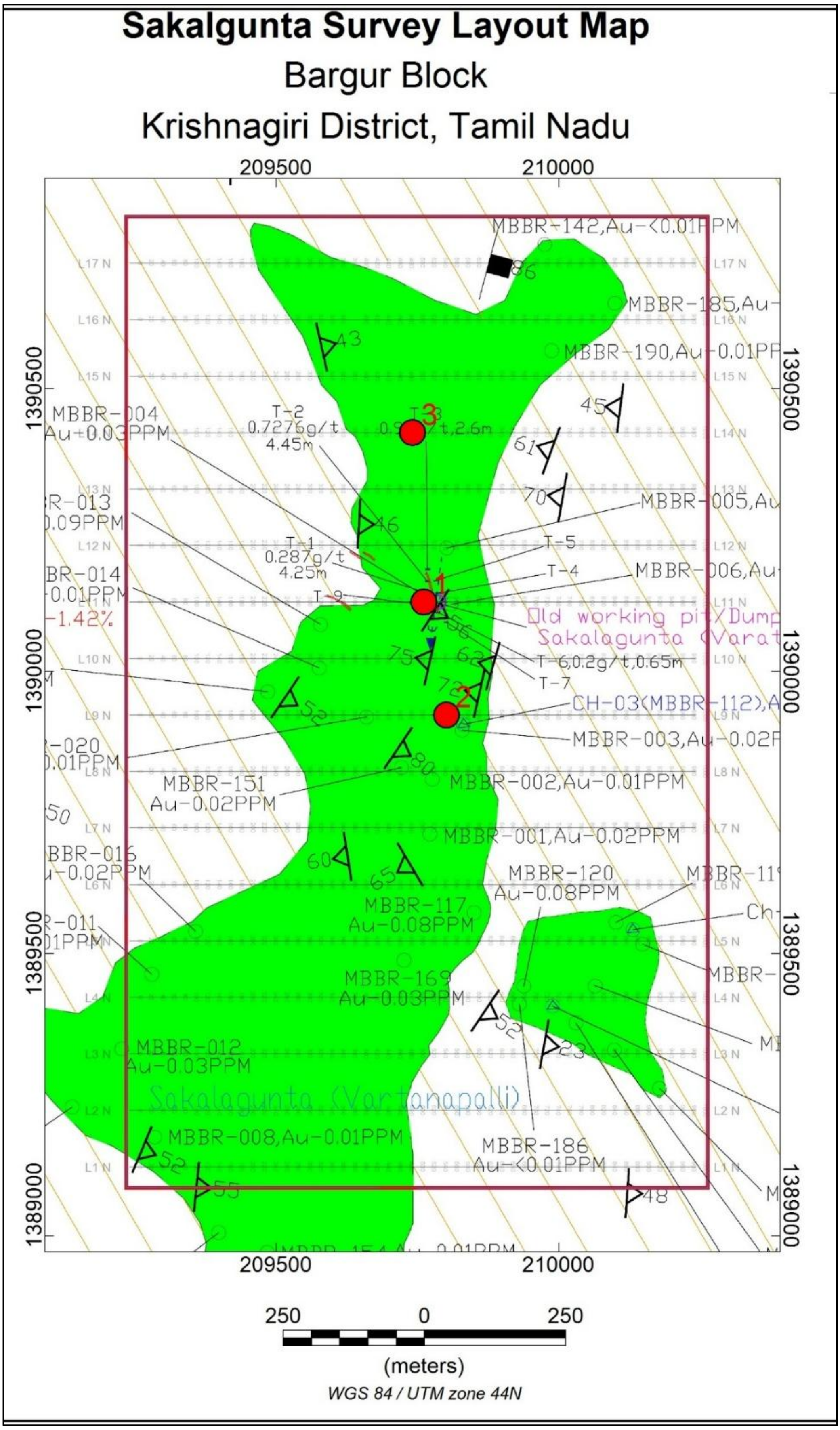

Fig. 6.1.1.8: Integrated Interpretation Map showing Proposed Borehole inferred location at Block-I (Sakalagunta) of Bargur Block.

Block-I (Sakalagunta) of Bargur Block.
2D Section of Resistivity and Chargeability

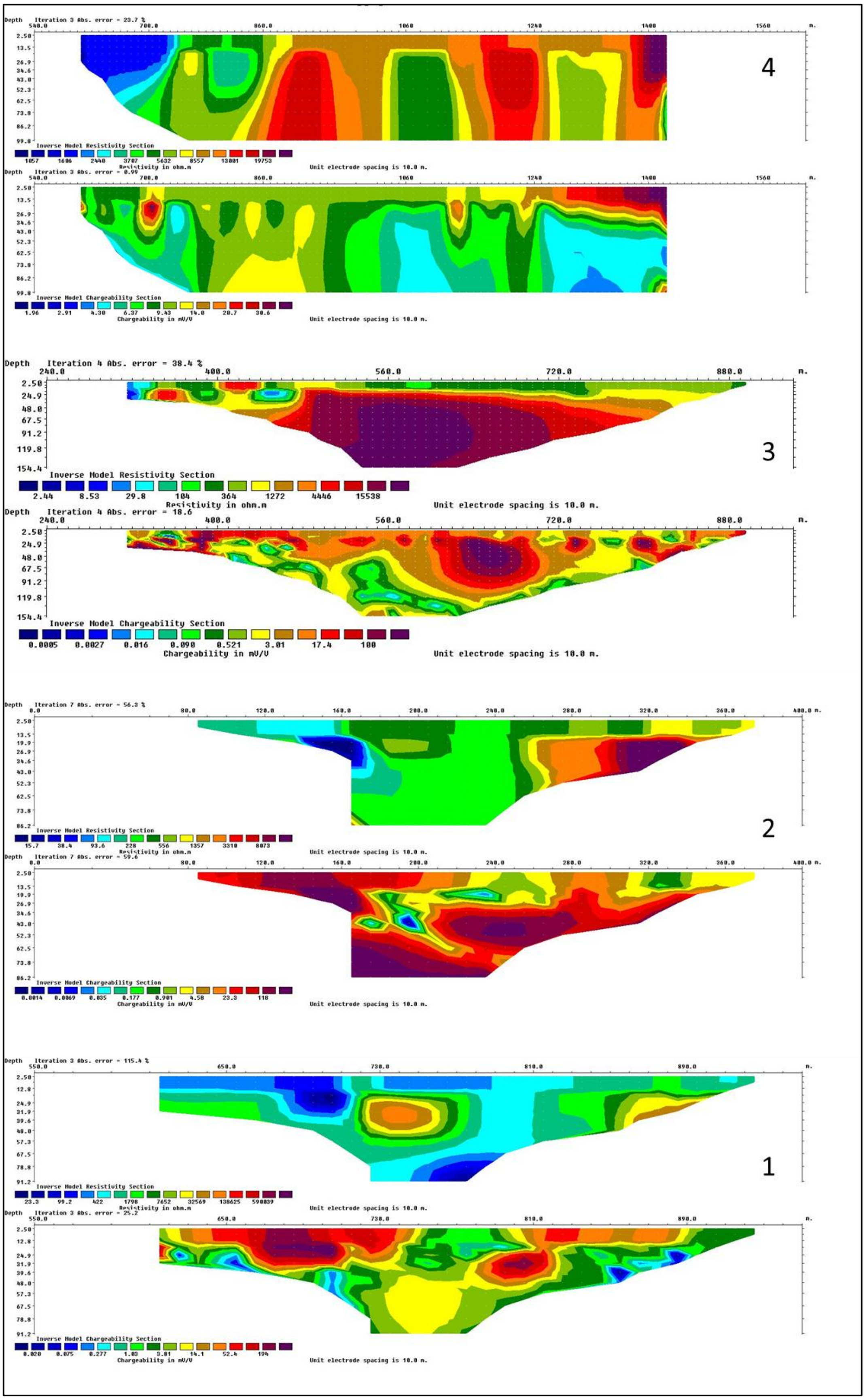

Fig. 6.2.1.1: 2D Section of Resistivity and Chargeability (Line 1 to 04) of Block-I

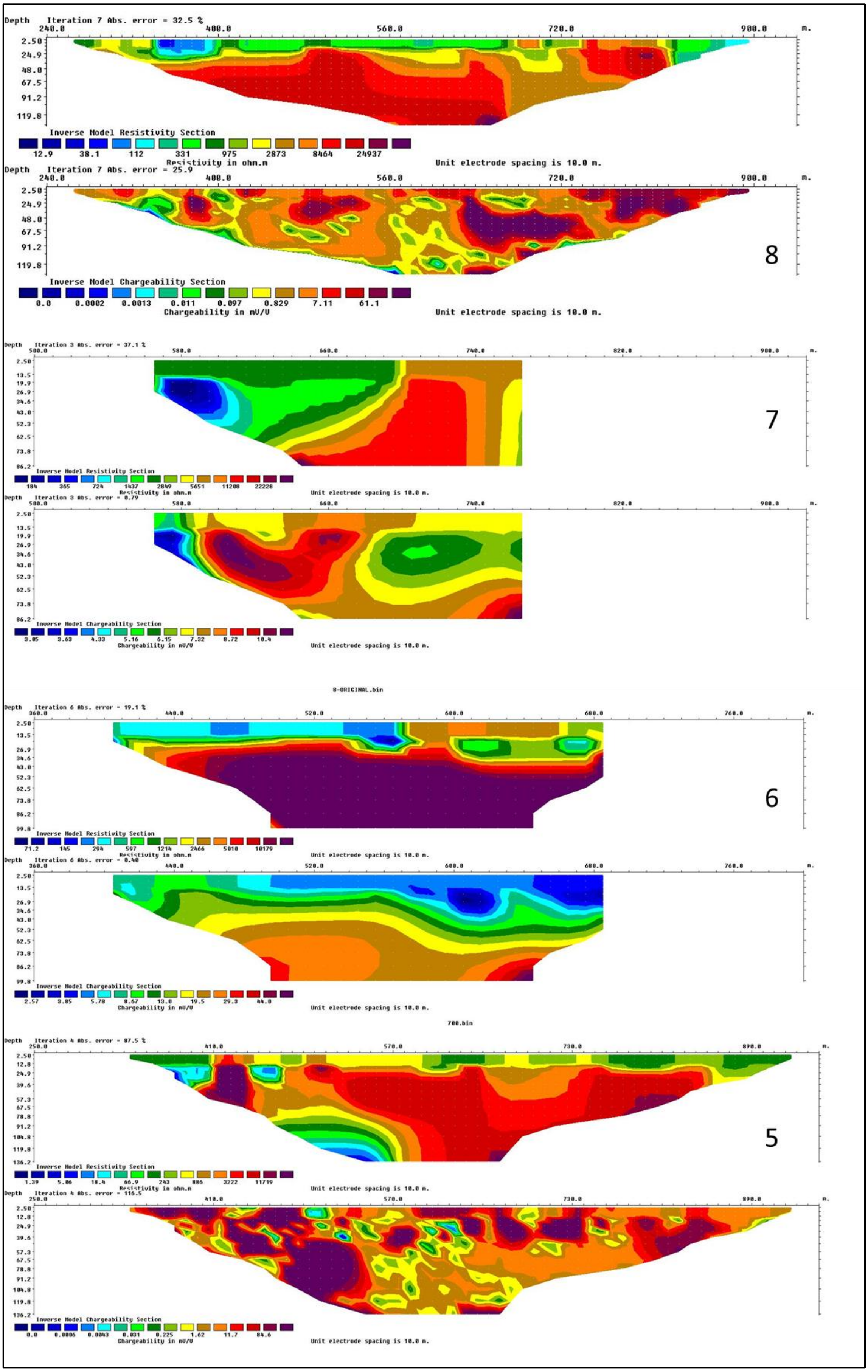

Fig. 6.2.1.2: 2D Section of Resistivity and Chargeability (Line 5 to 8) of Block-I

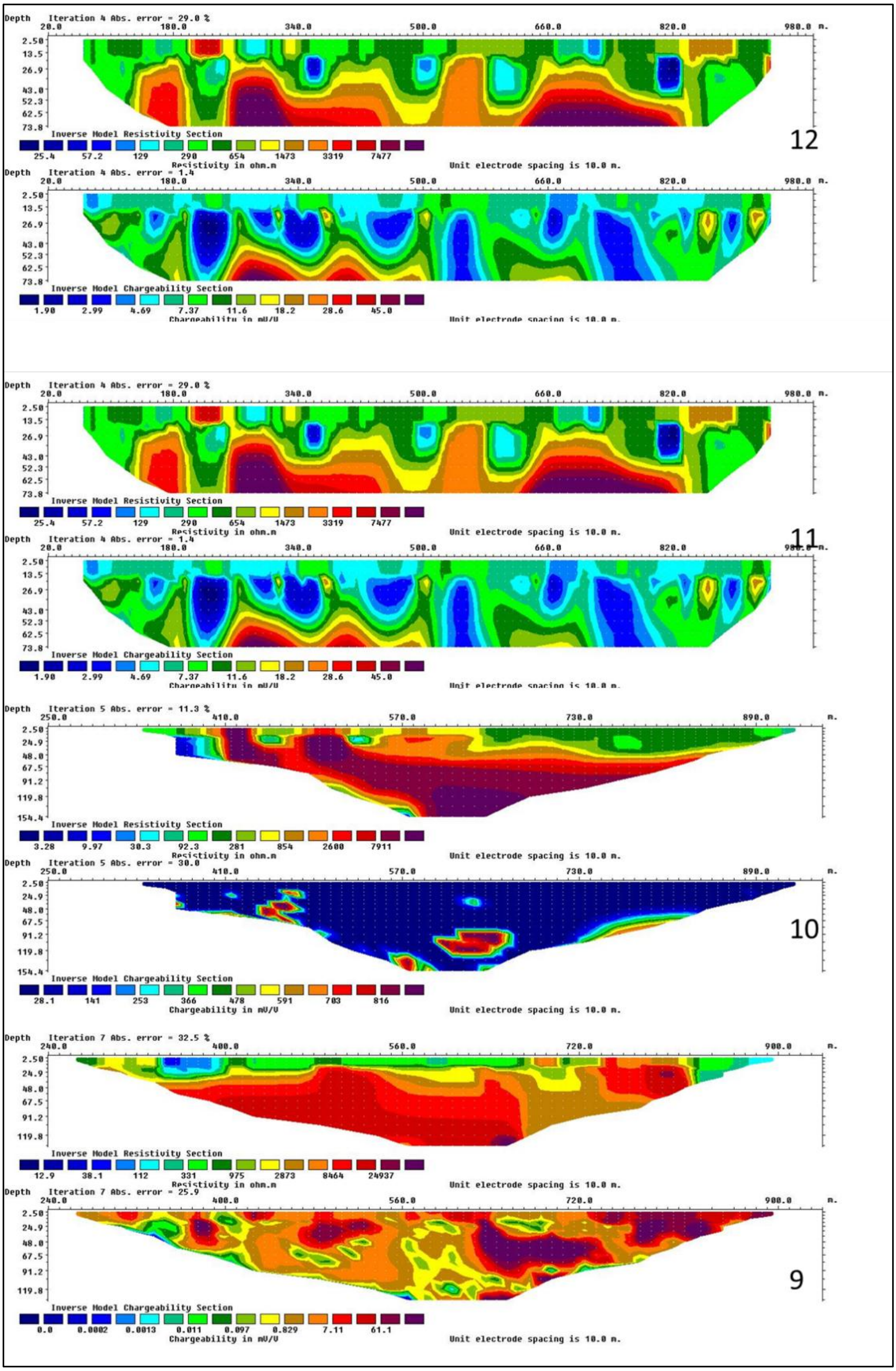

Fig. 6.2.1.3: 2D Section of Resistivity and Chargeability (Line 09 to 12) of Block-I

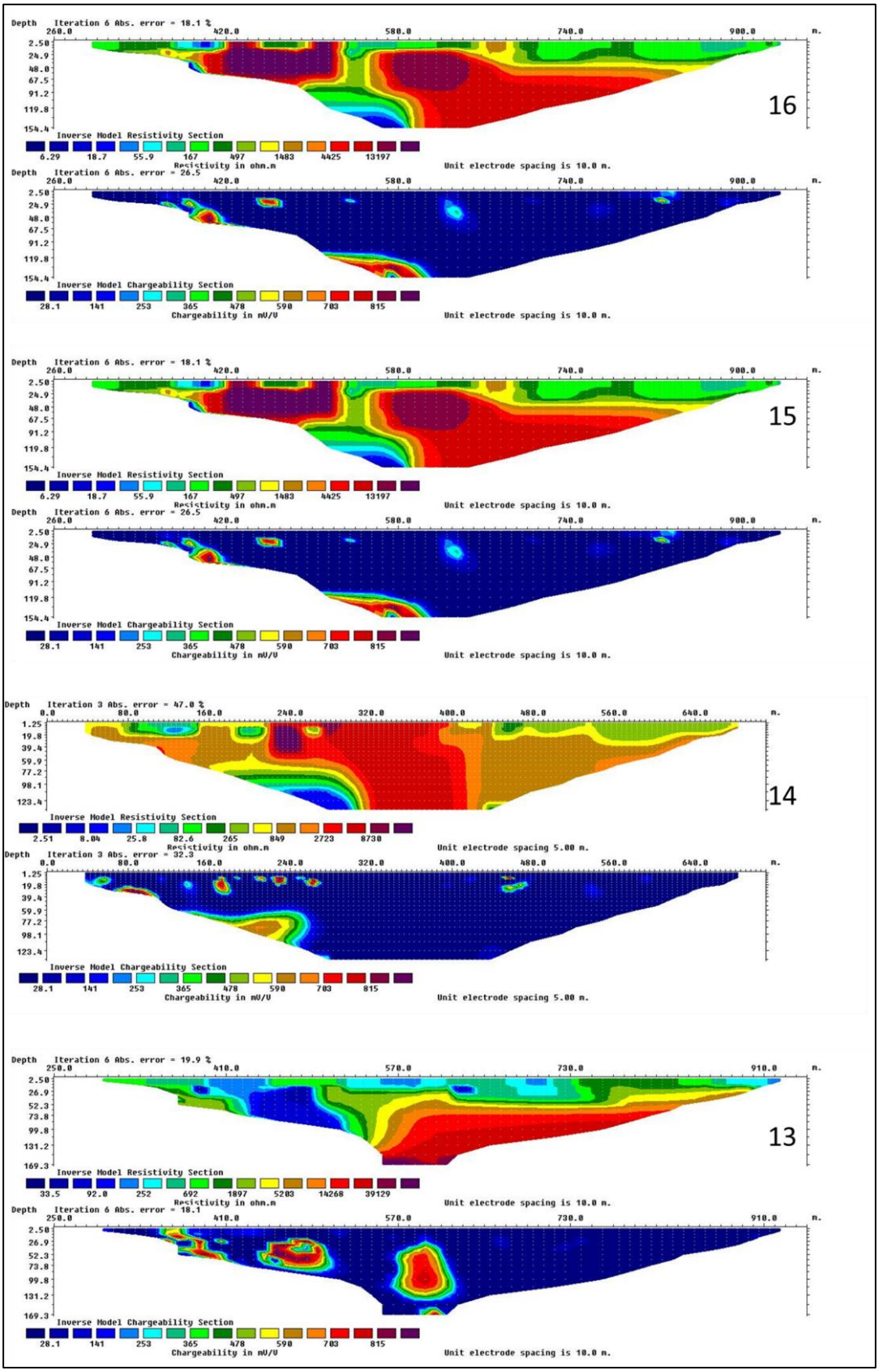

Fig.6.2.1.4: 2D Section of Resistivity and Chargeability (Line 13to 16) of Block-I

Block-II (Bangaragunta) of Bargur Block.

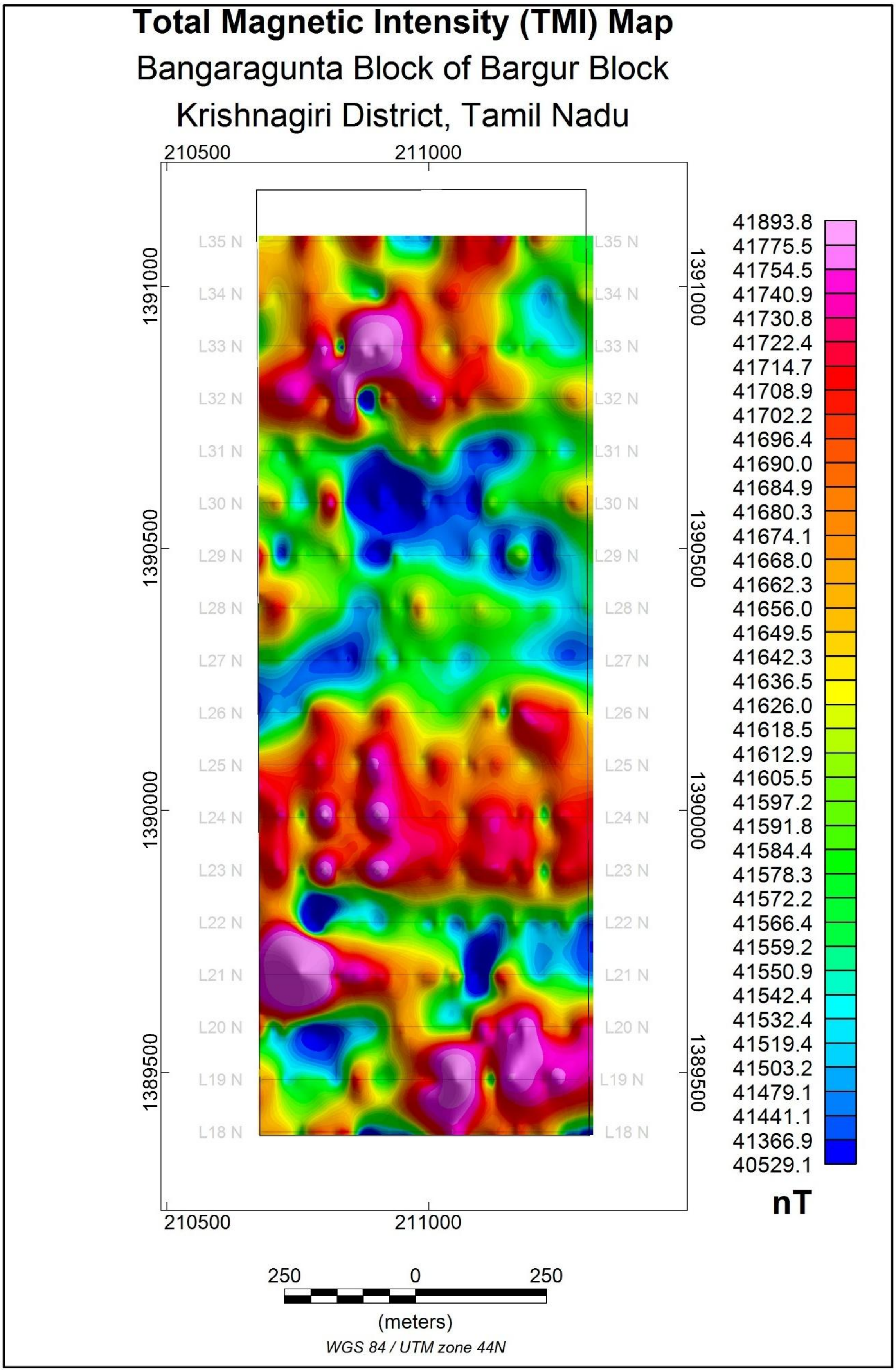

Fig. 6.1.2.1: Total Magnetic Intensity (TMI) Map of Block-II (Bangaragunta) of Bargur Block

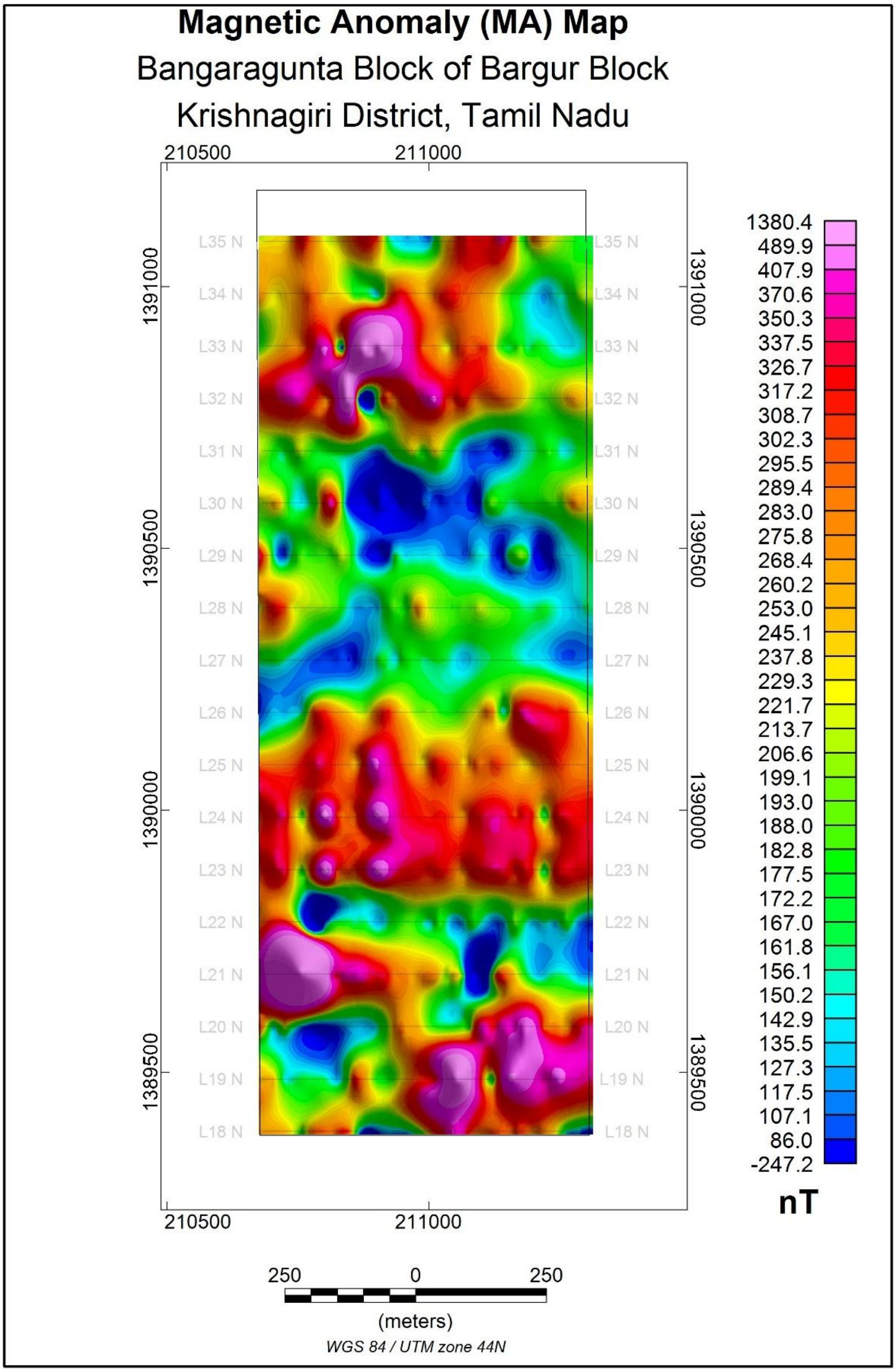

Fig. 6.1.2.2: Magnetic Anomaly (MA) Map of Block-II (Bangaragunta) of Bargur Block

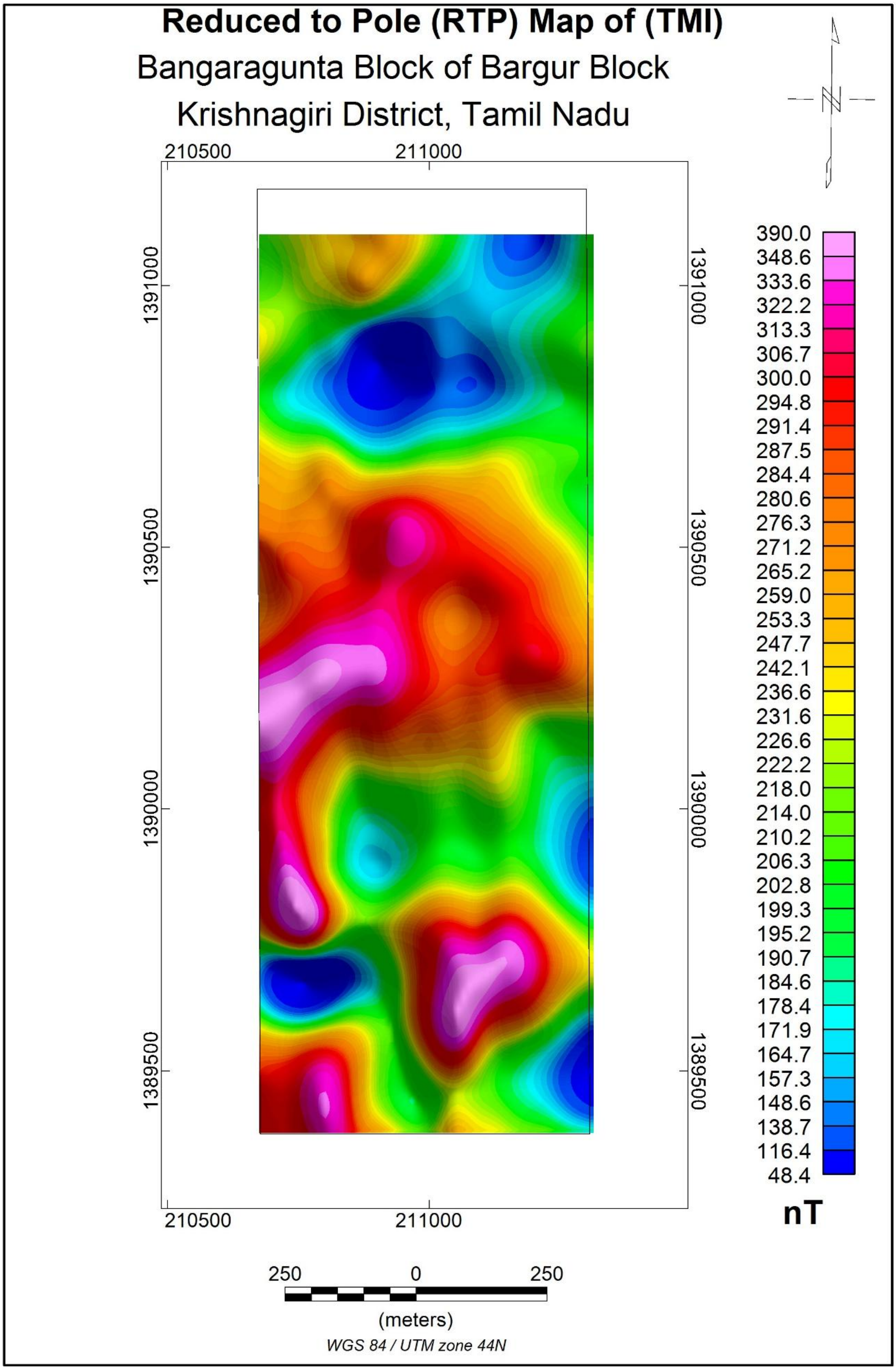

Fig. 6.1.2.3: Reduced to Pole (RTP) Map of (TMI) of Block-II (Bangaragunta) of Bargur Block

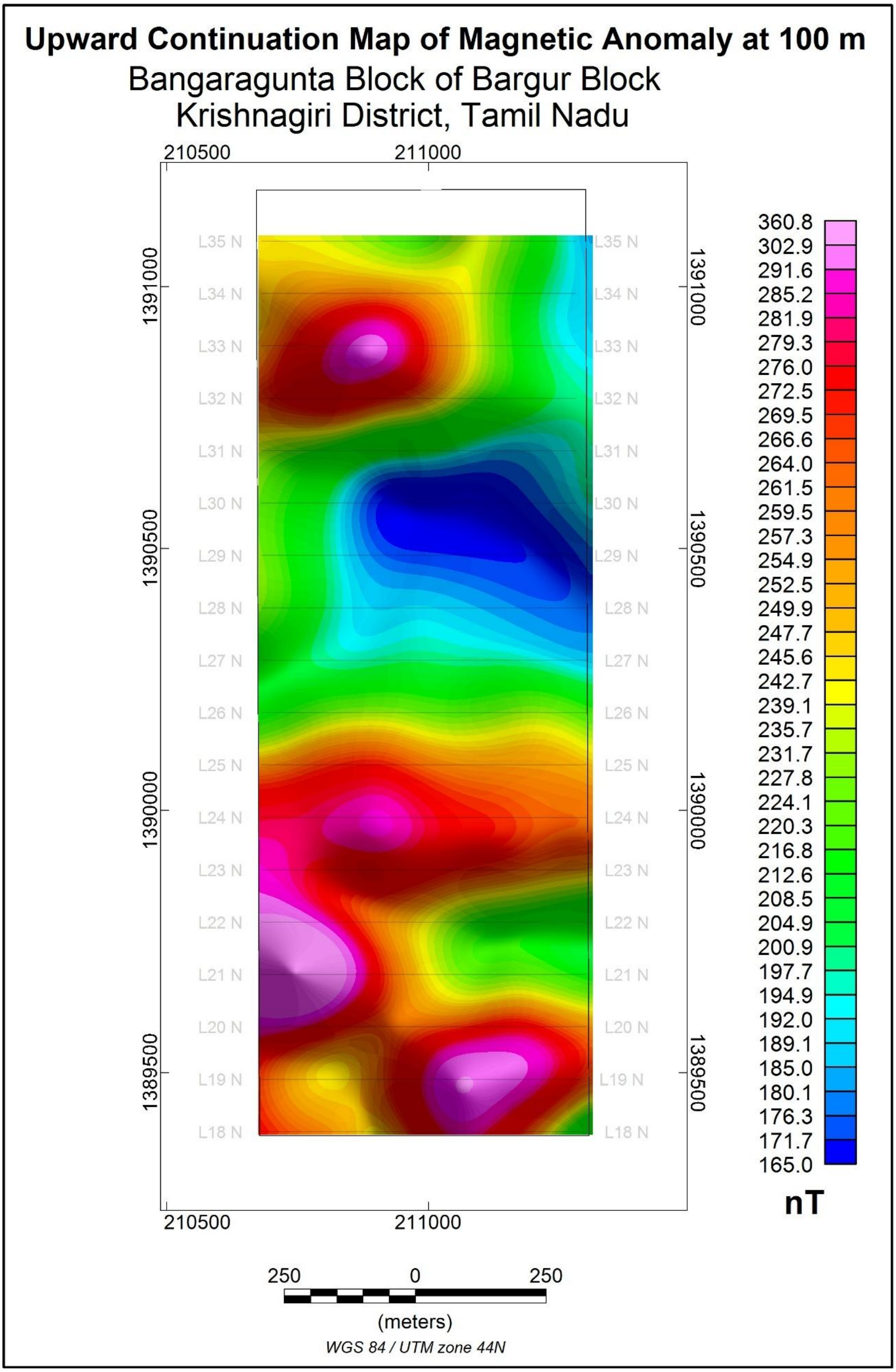

Fig. 6.1.2.4: Upward Continuation Map of Magnetic Anomaly at 100 m of Block-II (Bangaragunta) of Bargur Block

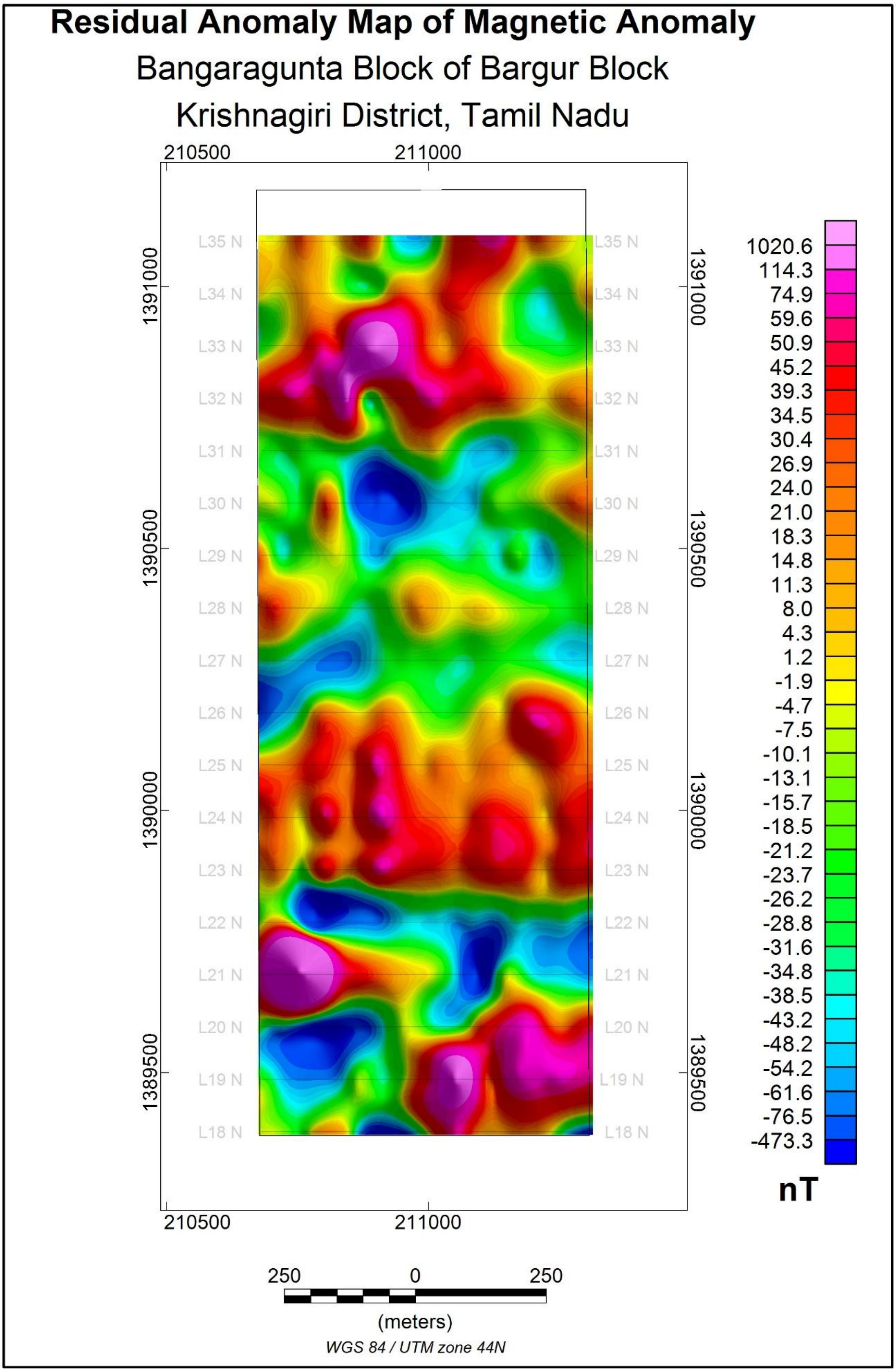

Fig. 6.1.2.5: Residual Anomaly Map of Magnetic Anomaly at 100 m of Block-II (Bangaragunta) of Bargur Block

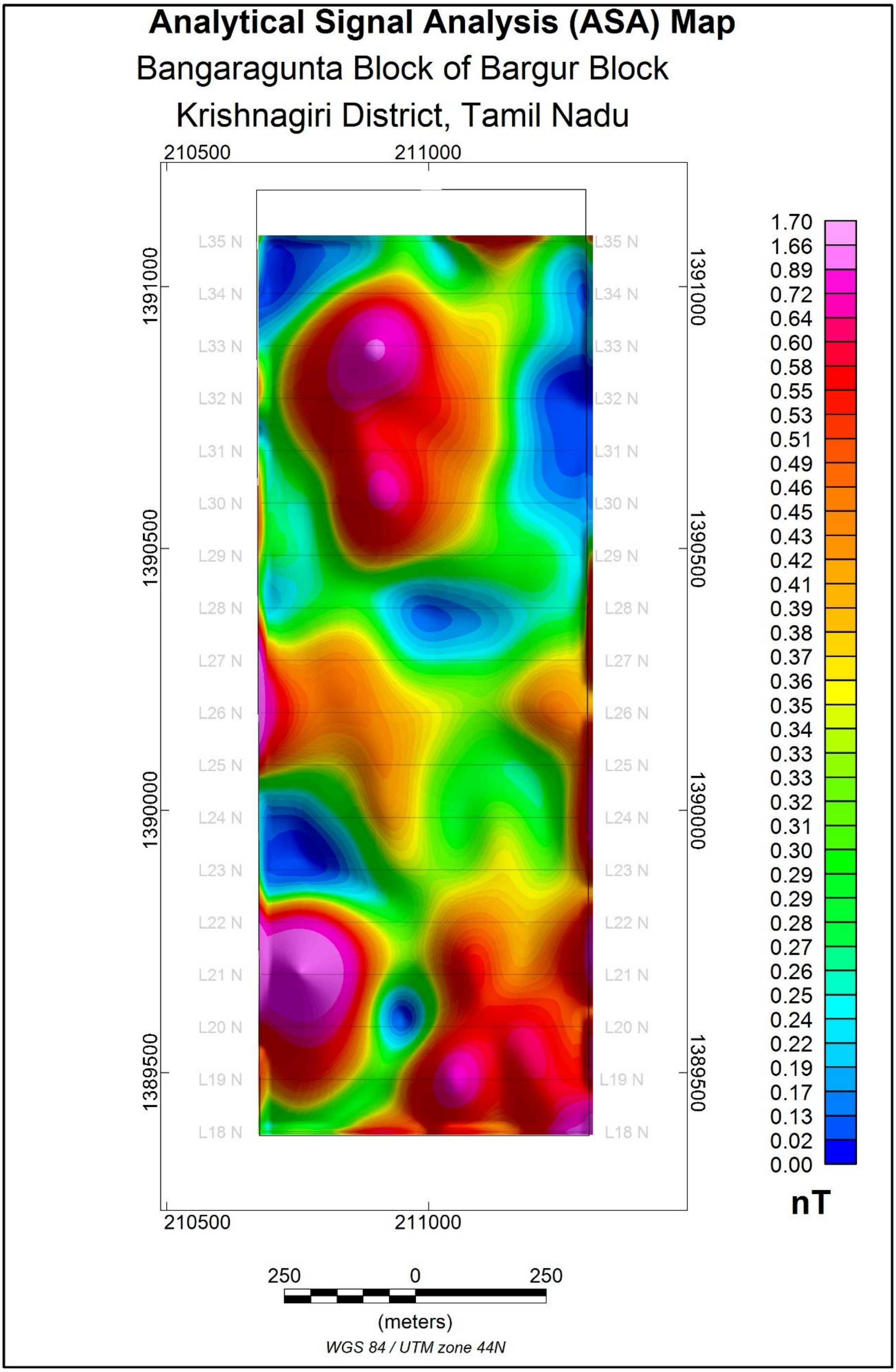

Fig. 6.1.2.6: Analytical Signal Analysis (ASA) Map of Block-II (Bangaragunta) of Bargur Block

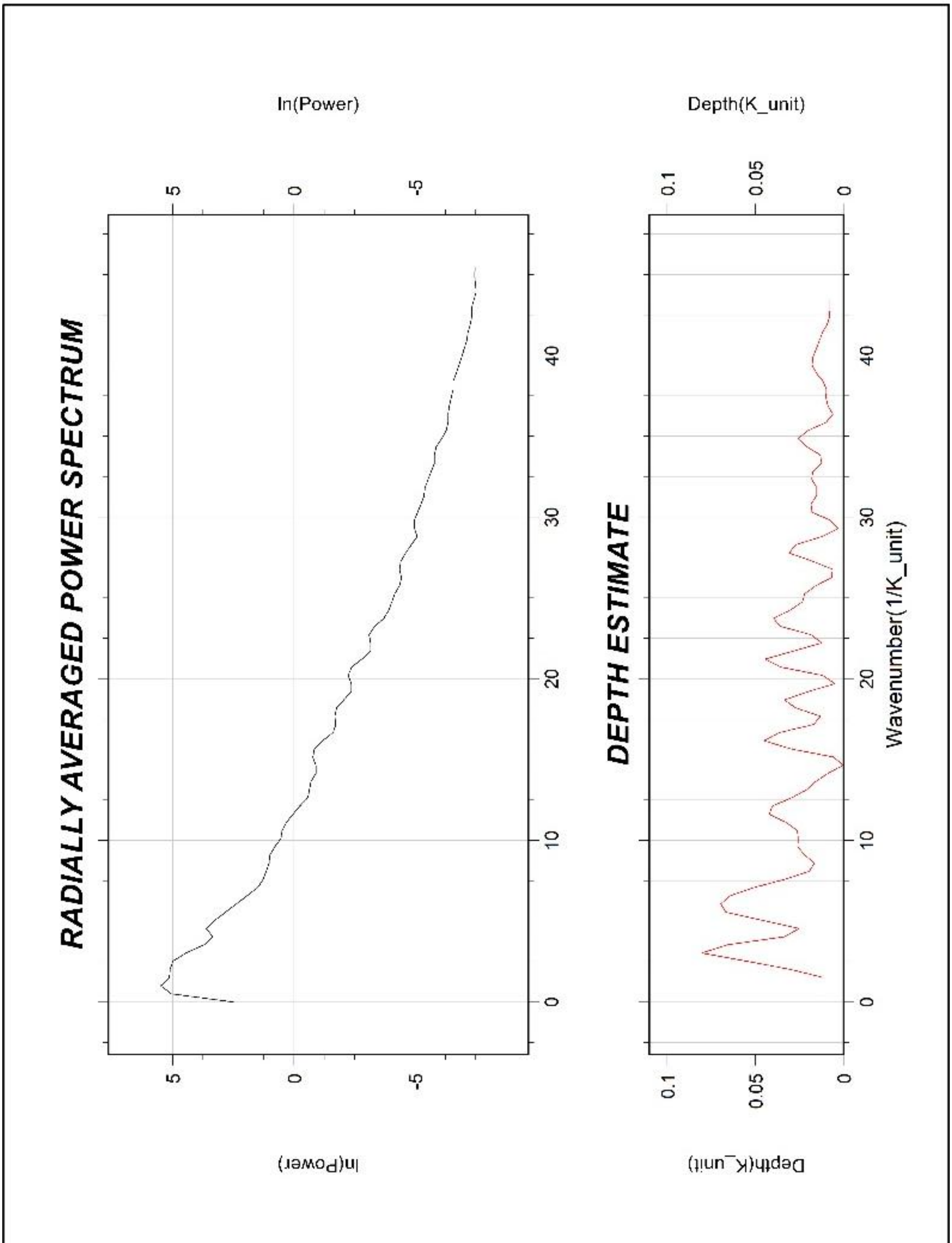

Fig. 6.1.2.7: Radially Average Power Spectrum of Block-II (Bangaragunta) of Bargur Block

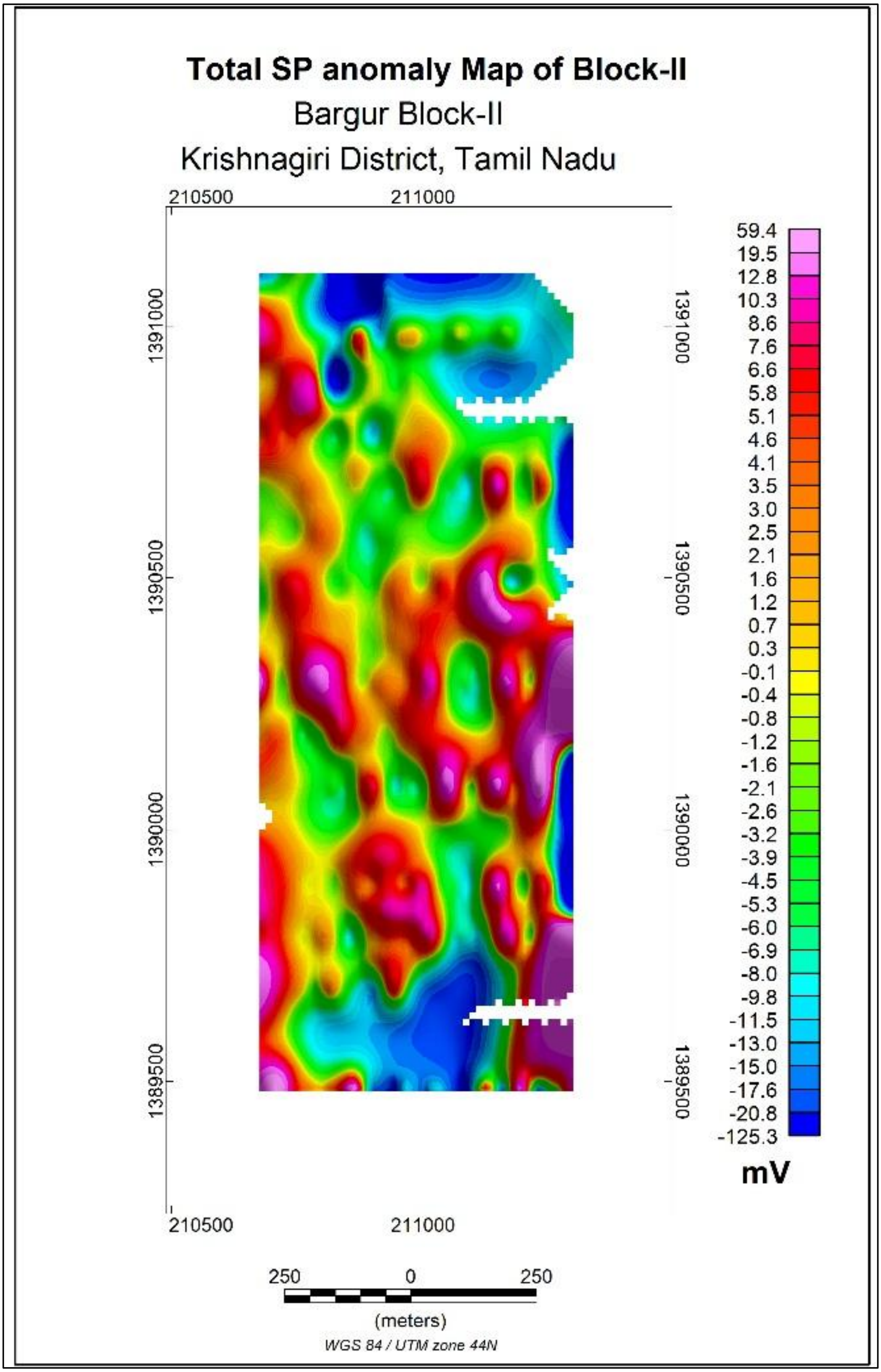

Fig. 6.1.2.8: Total SP anomaly Map of Block-II (Bangaragunta) of Bargur Block

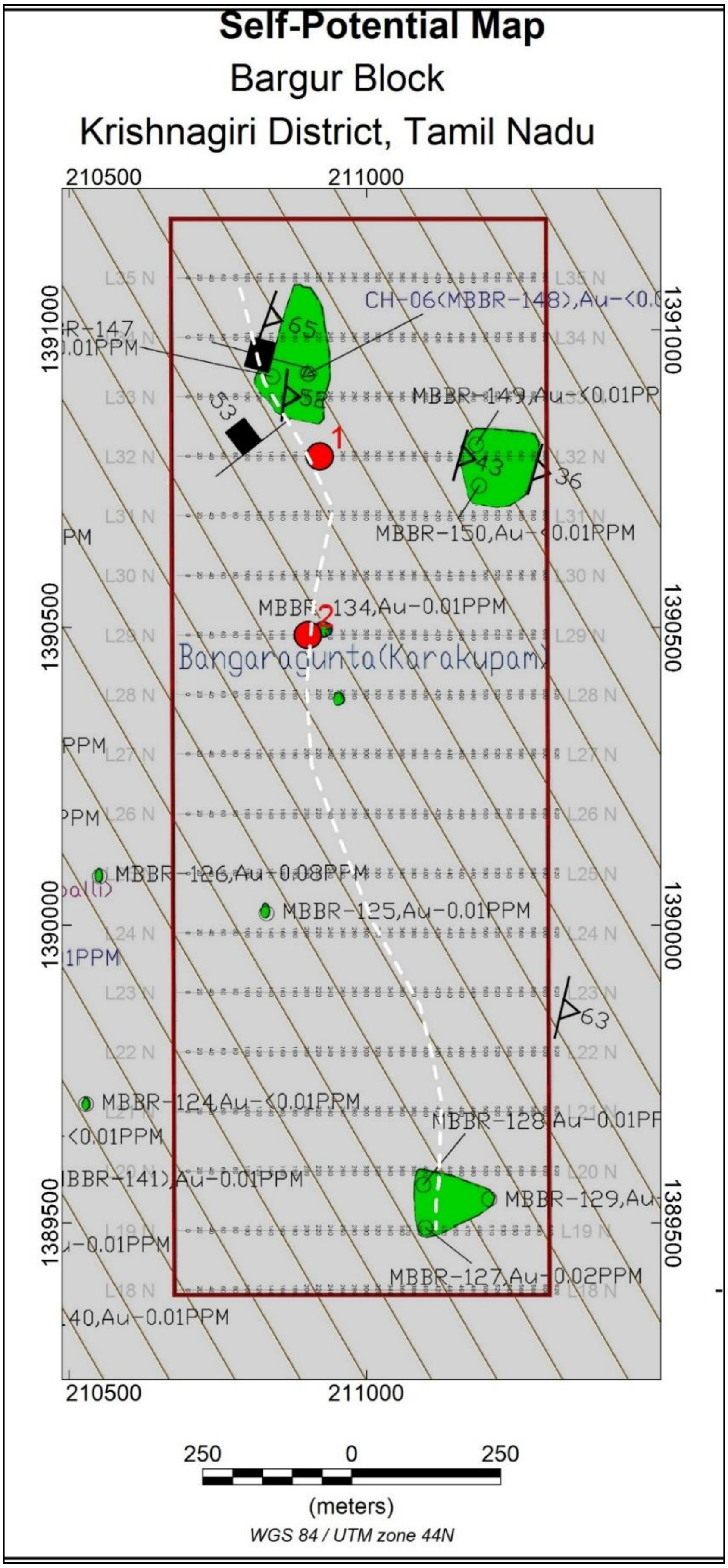

Fig. 6.2.2.9: Integrated Interpretation Map showing Proposed Borehole inferred location at Block-II (Bangaragunta) of Bargur Block of Bargur Block.

Block-II (Bangaragunta) of Bargur Block
2D Section of Resistivity and Chargeability

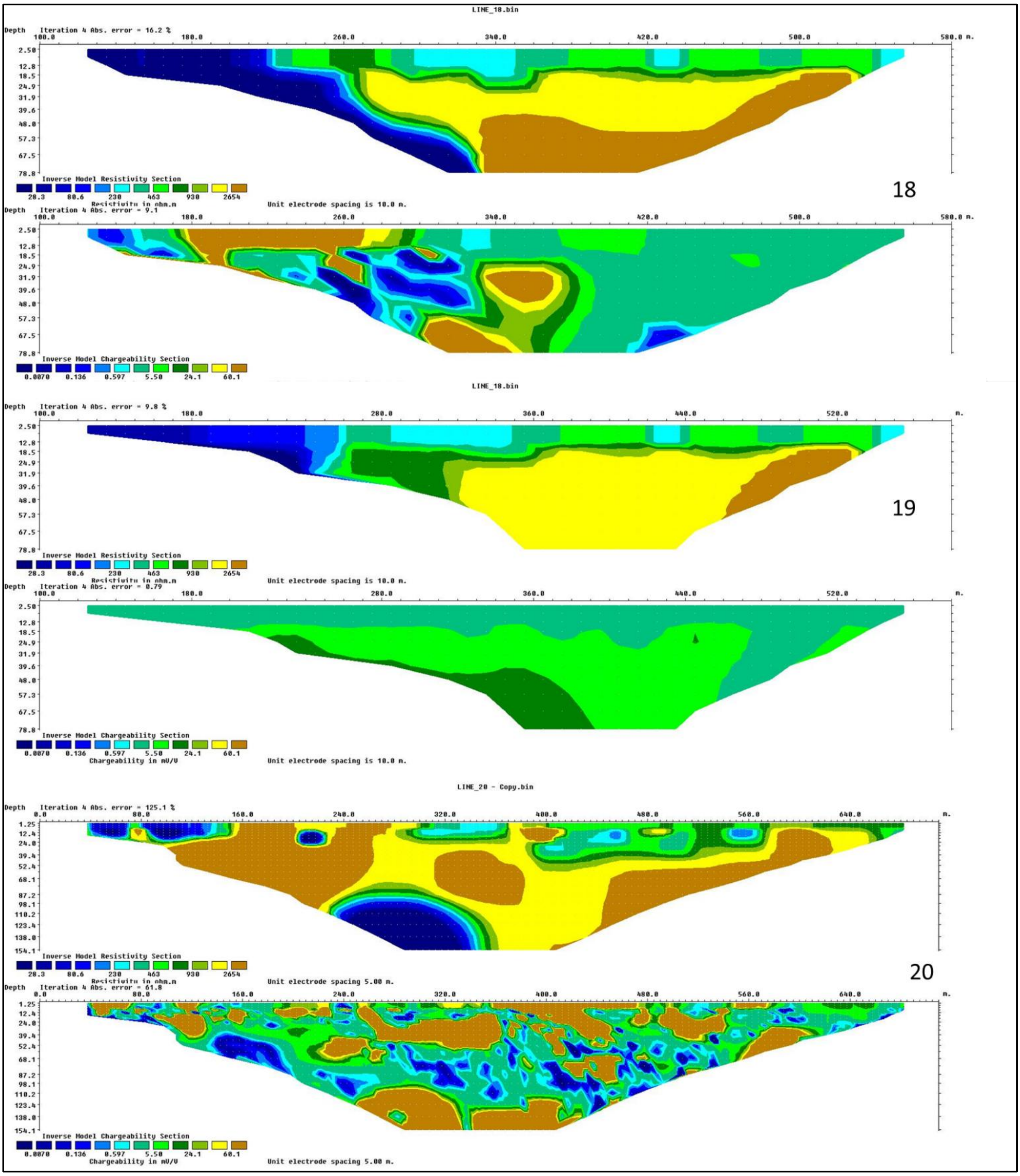

Fig. 6.2.2.1: 2D Section of Resistivity and Chargeability (Line 18 to 20) of Block-II (Bangaragunta) of Bargur Block

.

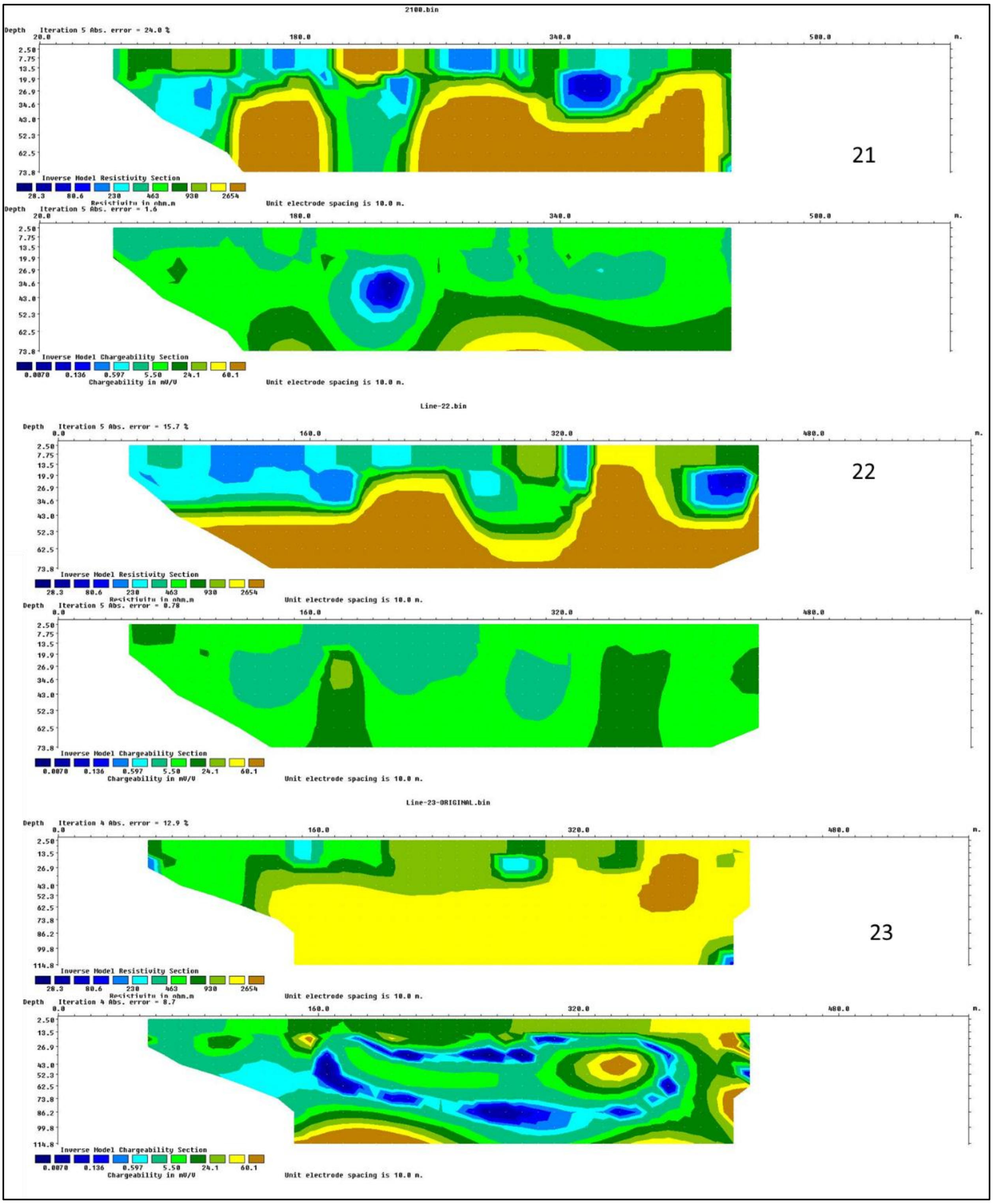

Fig. 6.2.2.2: 2D Section of Resistivity and Chargeability (Line 21 to 23) of Block-II (Bangaragunta) of Bargur Block

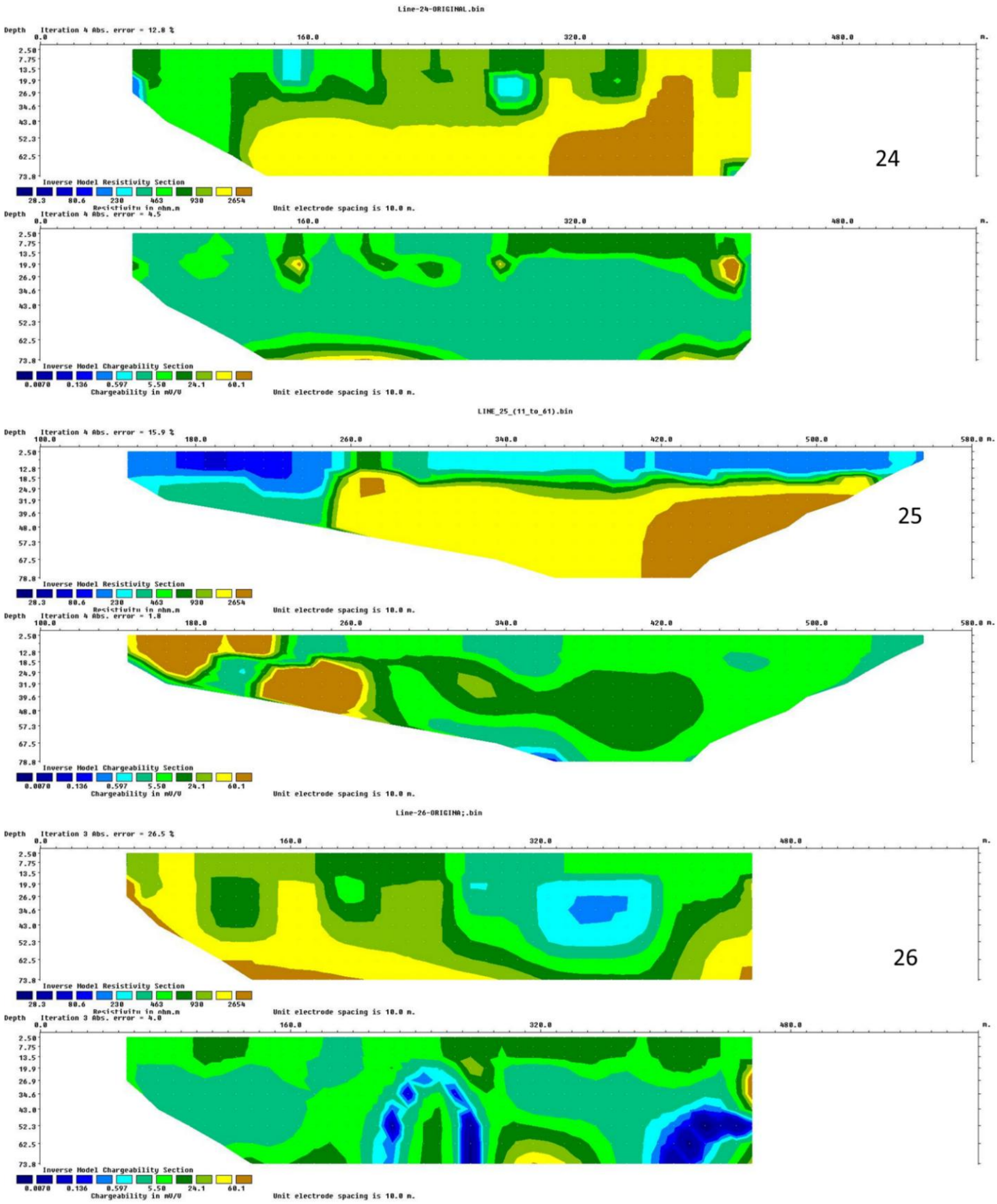

Fig. 6.2.2.3: 2D Section of Resistivity and Chargeability (Line 24 to 26) of Block-II (Bangaragunta) of Bargur Block

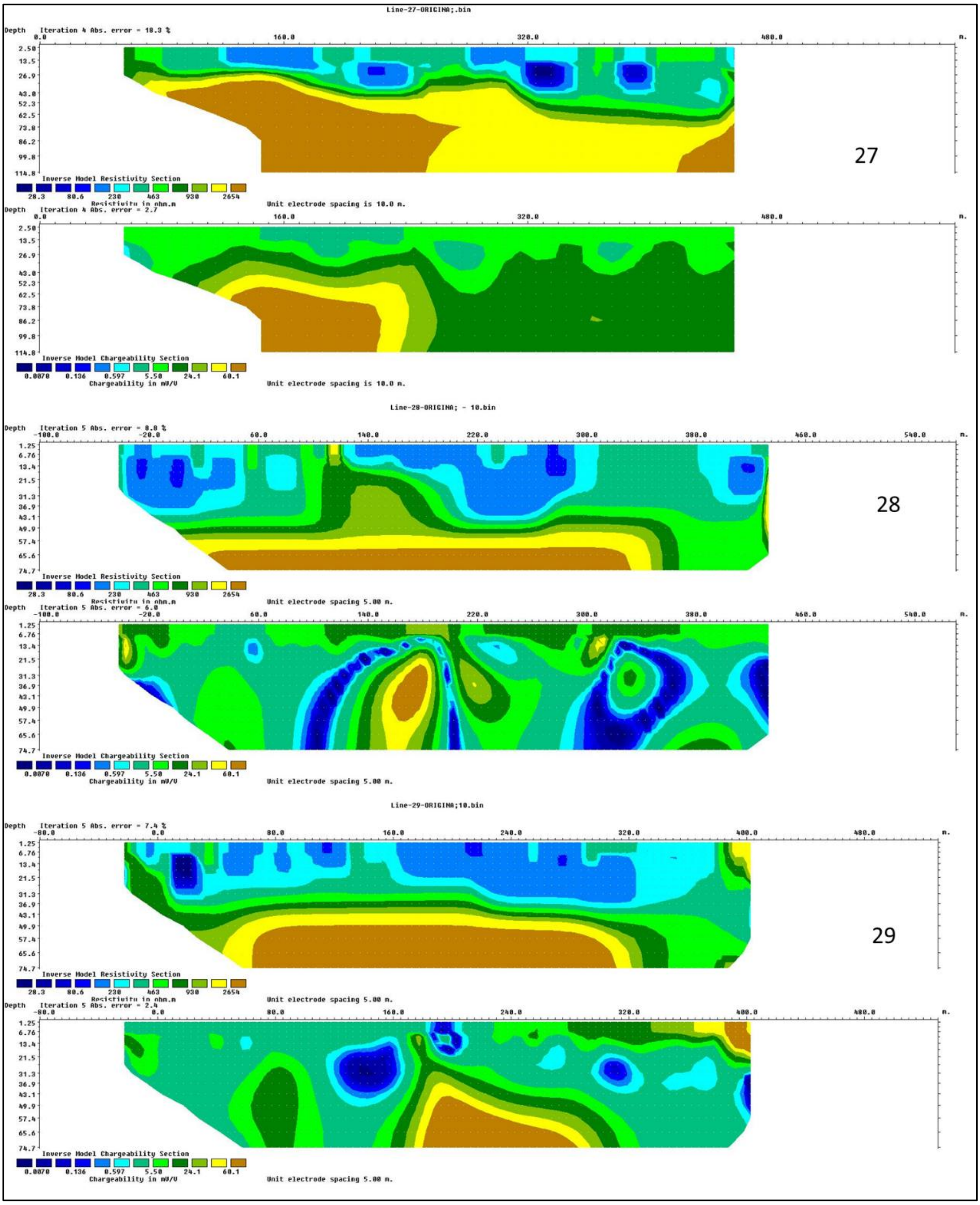

Fig. 6.2.2.4: 2D Section of Resistivity and Chargeability (Line 27 to 29) of Block-II (Bangaragunta) of Bargur Block

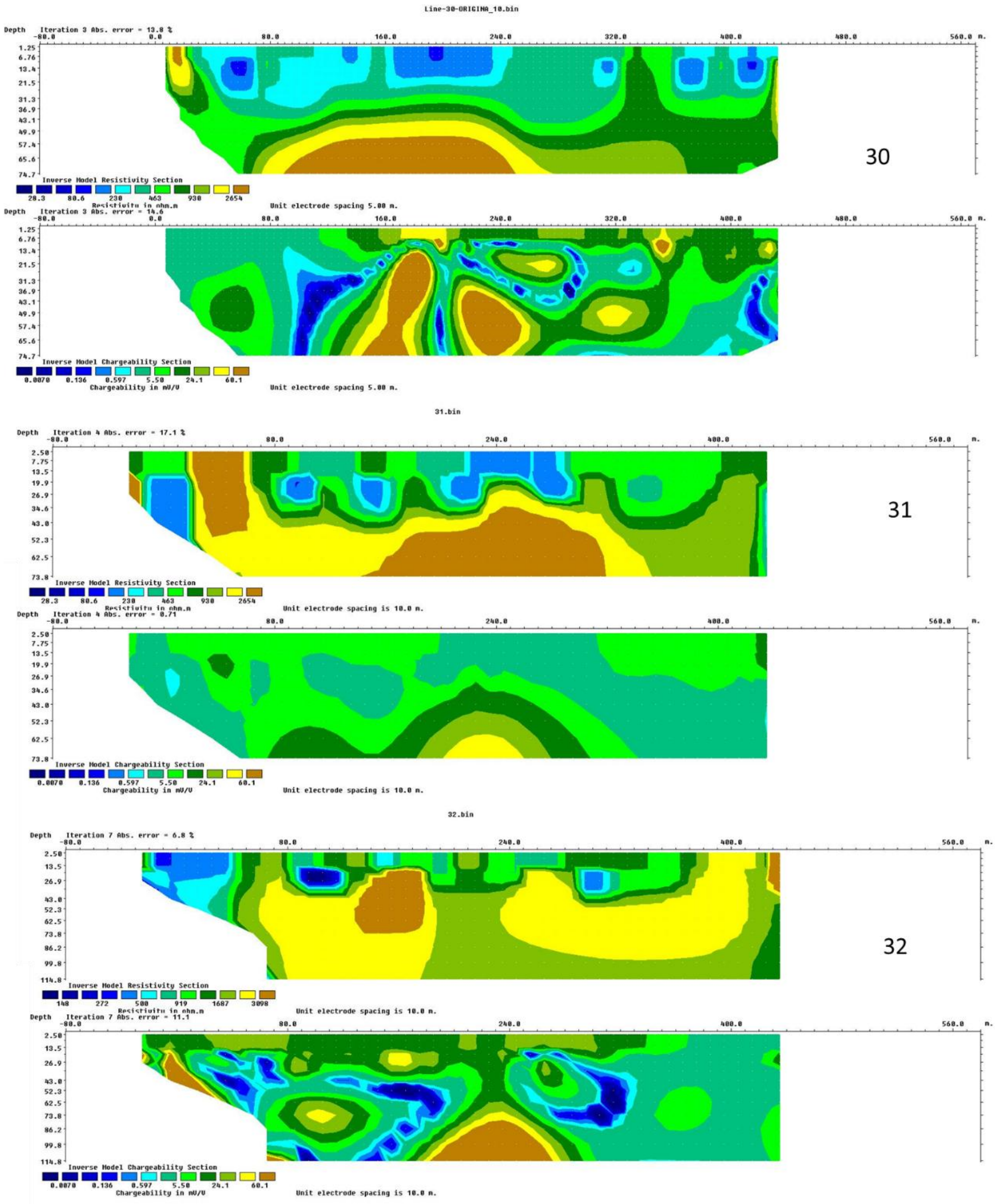

Fig. 6.2.2.5: 2D Section of Resistivity and Chargeability (Line 30 to 32) of Block-II (Bangaragunta) of Bargur Block

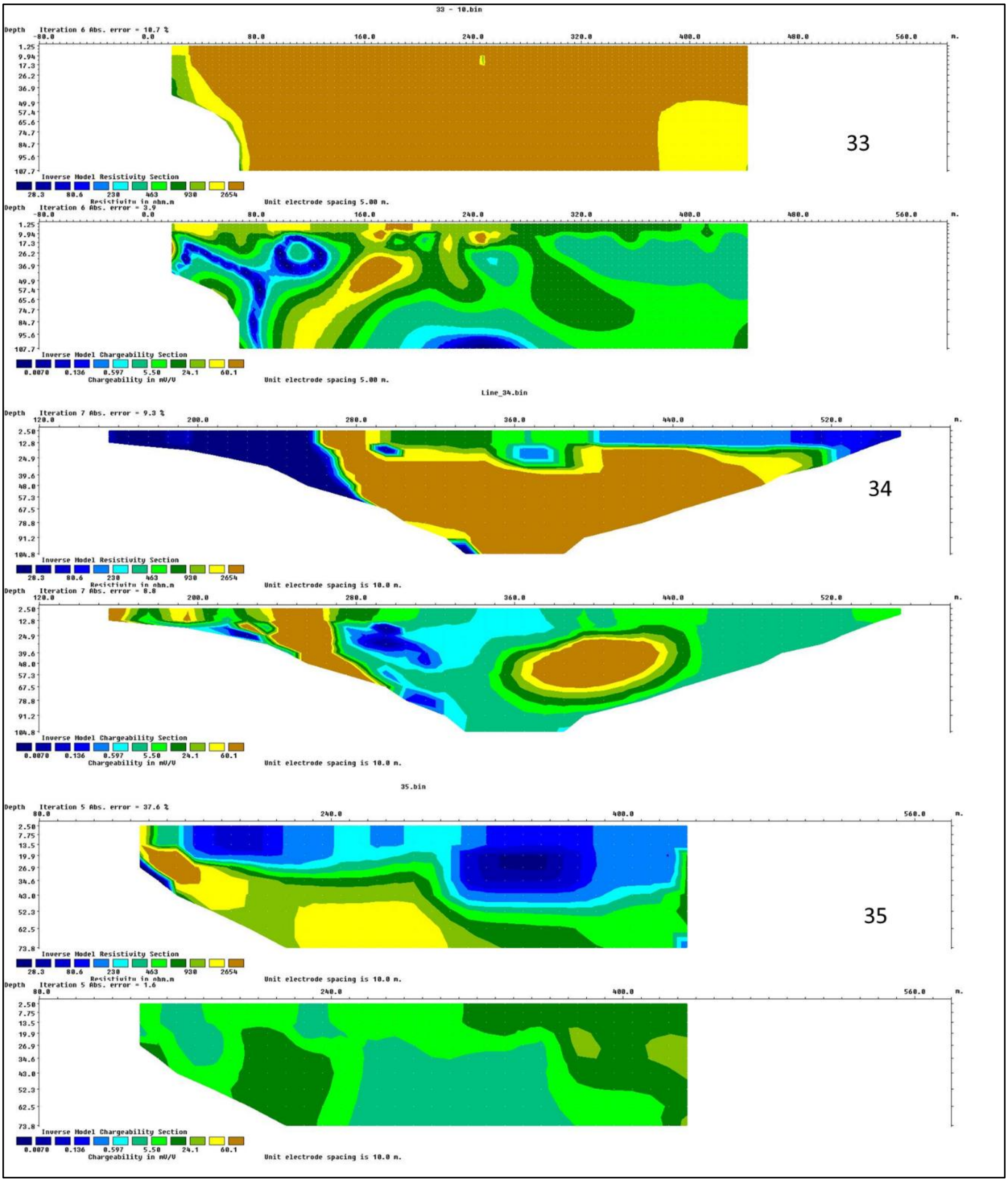

Fig. 6.2.2.6: 2D Section of Resistivity and Chargeability (Line 33 to 35) of Block-II (Bangaragunta) of Bargur Block

*****